

# Towards a variational Jordan-Lee-Preskill quantum algorithm

Junyu Liu<sup># 1, 2, 3, 4, 5, \*</sup> Jinzhao Sun<sup># 6, †</sup> and Xiao Yuan<sup>7, 8</sup>

<sup>1</sup>Walter Burke Institute for Theoretical Physics, California Institute of Technology, Pasadena, CA 91125, USA

<sup>2</sup>Institute for Quantum Information and Matter,

California Institute of Technology, Pasadena, CA 91125, USA

<sup>3</sup>Pritzker School of Molecular Engineering, The University of Chicago, Chicago, IL 60637, USA

<sup>4</sup>Chicago Quantum Exchange, Chicago, IL 60637, USA

<sup>5</sup>Kadanoff Center for Theoretical Physics, The University of Chicago, Chicago, IL 60637, USA

<sup>6</sup>Clarendon Laboratory, University of Oxford, Parks Road, Oxford OX1 3PU, United Kingdom

<sup>7</sup>Center on Frontiers of Computing Studies, Peking University, Beijing 100871, China

<sup>8</sup>Stanford Institute for Theoretical Physics, Stanford University, Stanford, CA 94306, USA

(Dated: September 30, 2021)

Rapid developments of quantum information technology show promising opportunities for simulating quantum field theory in near-term quantum devices. In this work, we formulate the theory of (time-dependent) variational quantum simulation, explicitly designed for quantum simulation of quantum field theory. We develop hybrid quantum-classical algorithms for crucial ingredients in particle scattering experiments, including encoding, state preparation, and time evolution, with several numerical simulations to demonstrate our algorithms in the 1+1 dimensional  $\lambda\phi^4$  quantum field theory. These algorithms could be understood as near-term analogs of the Jordan-Lee-Preskill algorithm, the basic algorithm for simulating quantum field theory using universal quantum devices. Our contribution also includes a bosonic version of the unitary coupled cluster ansatz with physical interpretation in quantum field theory, a discussion about the subspace fidelity, a comparison among different bases in the 1+1 dimensional  $\lambda\phi^4$  theory, and the “spectral crowding” in the quantum field theory simulation.

#: corresponding authors.

## I. INTRODUCTION

Quantum information science is currently an important direction of modern scientific research across several subjects, including quantum physics, computer science, information technology, and quantum engineering. The rapid development of quantum technology brings us evidence that quantum computers in the near-term are able to perform some specifically scientific computations using dozens of qubits, but errors appearing in the noisy quantum circuits might set certain limits of the computational scale [1, 2]. At the current stage, it makes sense to assume a reasonable quantum device exists and study potential scientific applications of such a device. This forms one of the main topics in the modern research of quantum information science.

Among numerous quantum applications, physicists, in particular, might care about how quantum devices could enlarge the range of computational capacity on certain problems in fundamental physics. In modern physics, quantum field theory is a general language or paradigm for describing almost all phenomena existing in the world, from sub-atomic particle physics, string theory and gravity, to condensed-matter and cold-atomic physics. If we

could imagine the existence of powerful quantum computers, it will be natural, important, and interesting to consider if quantum computation could address open problems appearing in the study of quantum field theories, where many of them are at strong coupling and strong correlation. In fact, simulating quantum field theories in quantum devices is one of the earliest motivations of quantum computation [3], and becomes an important new research direction recently in the physics community, see the references [4–7] as examples.

When simulating quantum field theories, or more generally, solving some well-defined computational tasks using quantum computation, theorists will either assume a universal, fault-tolerant quantum computer, or a noisy, near-term quantum circuit without enough quantum error correction. Both of them are wise choices and important scientific directions. Using fault-tolerant quantum computing is helpful for theoretical, conceptual problems or development of quantum devices usually appearing in the long-term, while studying near-term, early quantum computation will allow us to use existing machines and do experiments. In this paper, we will focus on the second direction, by exploring how far quantum simulation could go using near-term devices, with the help of specific problems in quantum field theories. It is helpful to see the usage and limitations of the currently existing, or future possible quantum hardware to simulate quantum field theories, and benchmark our quantum devices using interesting problems in fundamental physics [8]. Eventually, we believe that a universal, fault tolerant quantum device will come true, and we believe that our work might be helpful to speed up the process.

---

\* junyuli@uchicago.edu

† jinzhao.sun@physics.ox.ac.uk

Here, we are specifically looking at the Jordan-Lee-Preskill scattering problem [6, 7] in the 1+1 dimensional  $\lambda\phi^4$  quantum field theory. The research about scattering problems has a long history in physics, from the scattering experiment of alpha particles by Rutherford to the modern discovery of the Higgs boson. Performing scattering experiments and determining scattering matrices are important themes in particle physics and quantum field theories. In Refs. [6, 7], Jordan, Lee, and Preskill designed a full algorithm running in a universal quantum computer to perform particle scattering in quantum field theories, containing initial state preparation, time evolution, and measurement, where the proof of polynomial complexity is presented. In this work, we will construct closely-related algorithms that are more suitable for near-term quantum computers.

We will be most interested in the circumstance where we have a machine to perform variational quantum simulation and hybrid quantum-classical calculations (see, for instance, Refs. [9–18]). In those algorithms, we will imagine that quantum gates or states are parametrized by a few parameters, and we iteratively perform measurements from quantum states and construct variational algorithms to optimize those parameters. We believe that those algorithms realized in the laboratory might be able to perform useful computations and could tell us something unknown about fundamental physics.

In this work, we will systematically evaluate the possibility of variational quantum simulation in the context of  $\lambda\phi^4$  quantum field theory. We summarize our contribution as follows.

- **Basis choice.** We will make comments on the comparisons between the field basis and the harmonic oscillator basis, momentum space, and coordinate space. All those choices have pros and cons. Coordinate space setup will make the Lagrangian density local, but it is not directly connected to the Feynmann rules and scattering calculations in the momentum space. The momentum space setup is not local but still sparse, leaving a door open for variational (and also digital) simulations. The harmonic oscillator basis is easy to formulate, track, and identify the energy levels of states, but may not be easy to identify field profiles. The field basis will cause the field correlations to be easy to measure, but finding the eigenstates (for instance, the vacuum and low-lying one-particle states) might be not easy (which requires computing correlation functions at hand and non-trivial digital quantum algorithms for encoding).
- **Initial state preparation.** In order to prepare the initial wave packets, the original Jordan-Lee-Preskill algorithm uses adiabatic state preparation to turn on the coupling. In the variational setup, alternative strategies could be directly used and solve the initial scattering directly. In this work, we will discuss possible variational algorithms in

detail, especially on the treatment of the momentum sectors. Specifically, we perform numerical simulations using the imaginary time evolution [19] and a bosonic version of the unitary coupled cluster (UCC) ansatz with physical interpretation in quantum field theory [20–22] to test our simulation algorithms. We also theoretically and numerically investigate the spectral crowding phenomena in the quantum field theories in both weakly-coupled and strongly-coupled theories.

- **Real-time evolution and scattering.** Besides digital quantum simulation algorithms (see Refs. [23–27]), the real-time evolution algorithms could also be tracked by variational methods, see Refs. [12, 13, 28, 29]. In this work, we present the formulation of the corresponding algorithms, and discuss how to guarantee a certain simulation accuracy. We also comment on the particle excitations, circuit ansatz, and the challenges.
- **Simulation fidelity.** Simulation errors in the variational simulation will not only be limited to the digital simulation error (like the Trotter error) but also the variational error from the variational ansatz, measurement error, and noise in the devices. In this work, we observe that in the initial scattering state preparation, as long as the total particle number and type are not changed significantly, the scattering experiment could still be performed, even starting with imprecise wave packets. Thus, the task of scattering state preparation could tolerate more noise (where we could define particle subspace fidelity to quantify it), thus suitable for noisy intermediate-scale quantum (NISQ) devices. We numerically verify the fidelity in the one-particle subspace in the interacting theory. The real-time evolution task might require higher precision to make sure consistent scattering results, and we analyze the simulation error during the scattering process.

The paper is organized as the following. In Section II, we discuss the theoretical formulation of the  $\lambda\phi^4$  theory and the Jordan-Lee-Preskill algorithm, commenting on its variational extension. In Section III, we discuss different bases for state encoding and their comparisons. In Section IV, we discuss the variational initial state preparation in the Jordan-Lee-Preskill algorithm. In Section V, we discuss variational quantum simulation of the scattering dynamics, and analyze the simulation error during time evolution. We comment on the possibility of realizing the particle scattering process. In Section VI, we show the numerical simulation for the ground state and excited states preparation using variational quantum algorithms, and compare it with adiabatic evolution. We discuss the simulation results for different strength of the interacting field. Finally, in Section VII, we highlight a list of future directions.

## II. $\lambda\phi^4$ THEORY AND THE JORDAN-LEE-PRESKILL ALGORITHM

### A. Basics

In this section, we give a review of the  $\lambda\phi^4$  theory in 1+1 dimensions. In this theory, we have a scalar quantum field  $\phi$  with the Hamiltonian

$$H = \int dx \left( \frac{1}{2}\pi^2 + \frac{1}{2}(\partial_x\phi)^2 + \frac{1}{2}m_0^2\phi^2 + \frac{\lambda_0}{4!}\phi^4 \right),$$

and the Lagrangian

$$L = \int dx \left( \frac{1}{2}(\partial_t\phi)^2 - \frac{1}{2}(\partial_x\phi)^2 - \frac{1}{2}m_0^2\phi^2 - \frac{\lambda_0}{4!}\phi^4 \right).$$

Moreover, we discretize it in the lattice,

$$H = \sum_{x \in \Omega} a \left[ \frac{1}{2}\pi^2 + \frac{1}{2}(\nabla_a\phi)^2 + \frac{1}{2}m_0^2\phi^2 + \frac{\lambda_0}{4!}\phi^4 \right],$$

with the Lagrangian

$$L = \sum_{x \in \Omega} a \left[ \frac{1}{2}(\partial_t\phi)^2 - \frac{1}{2}(\nabla_a\phi)^2 - \frac{1}{2}m_0^2\phi^2 - \frac{\lambda_0}{4!}\phi^4 \right].$$

The theory is defined on a lattice  $\Omega$  with total length  $L$  and lattice spacing  $a$  as  $\Omega = a\mathbb{Z}_N$ , and  $N = \frac{L}{a}$ , and we could also define its dual lattice  $\Gamma = \frac{2\pi}{L}\mathbb{Z}_N$ . We use  $x$  to denote the sites in the lattice. The field momentum  $\pi(x)$  is defined as the Fourier conjugate of the field  $\phi(x)$ ,

$$\begin{aligned} \text{lattice: } [\phi(x), \pi(y)] &= ia^{-1}\delta_{x,y}, \\ \text{continuum: } [\phi(x), \pi(y)] &= i\delta(x-y). \end{aligned}$$

The discretized version of the derivative is given by  $(\nabla_a\phi)^2(x) = (\phi(x+a) - \phi(x))^2/a^2$ , where  $m_0$  is the (bare) mass term in the free theory, and the  $\frac{\lambda_0}{4!}\phi(x)^4$  term represents the coupling. When  $\lambda_0 = 0$ , we call it the free theory. In the case of the free theory, we could diagonalize the Hamiltonian by the following mode decomposition in the continuum,

$$\begin{aligned} \phi(x) &= \int \frac{dp}{2\pi} \sqrt{\frac{1}{2\omega_p}} (a_p + a_{-p}^\dagger) e^{ipx}, \\ \pi(x) &= -i \int \frac{dp}{2\pi} \sqrt{\frac{\omega_p}{2}} (a_p - a_{-p}^\dagger) e^{ipx}, \end{aligned} \quad (1)$$

and in the discrete system we have,

$$\begin{aligned} \phi(x) &= \sum_{p \in \Gamma} \frac{1}{L} e^{ipx} \sqrt{\frac{1}{2\omega(p)}} (a_p + a_{-p}^\dagger), \\ \pi(x) &= -i \sum_{p \in \Gamma} \frac{1}{L} e^{ipx} \sqrt{\frac{\omega(p)}{2}} (a_p - a_{-p}^\dagger), \end{aligned} \quad (2)$$

where the canonical algebra of  $\phi$  and  $\pi$  leads to the commutation relation as  $[a_p, a_q^\dagger] = L\delta_{p,q}$  for lattice and  $[a_p, a_q^\dagger] = 2\pi\delta(p - q)$  for continuum, respectively. The energy dispersion is given by

$$\omega(p) = \sqrt{m_0^2 + \frac{4}{a^2}\sin^2\left(\frac{ap}{2}\right)} \xrightarrow{a \rightarrow 0} \omega_p \equiv \sqrt{m_0^2 + p^2}. \quad (3)$$

In such a basis, the Hamiltonian is diagonalized as

$$H_0 = \sum_{p \in \Gamma} \frac{1}{L} \omega(p) a_p^\dagger a_p + E_0 \xrightarrow{a \rightarrow 0} \int \frac{dp}{2\pi} \omega_p a_p^\dagger a_p + E_0, \quad (4)$$

where

$$E_0 = \sum_{p \in \Gamma} \frac{1}{2} \omega(p) \xrightarrow{a \rightarrow 0} \int \frac{dp}{2\pi} \frac{1}{2} \omega_p \times 2\pi\delta(0). \quad (5)$$

An important physical observable we could measure, is the (Wightman) two-point function as  $G(x - y) = \langle \Omega | \phi(x)\phi(y) | \Omega \rangle$ , where  $|\Omega\rangle$  is the ground state of the theory. In the free theory case where  $\lambda_0 = 0$ , one can compute the two point function explicitly

$$G_0(x - y) = \sum_{p \in \Gamma} \frac{1}{L} \frac{1}{2\omega(p)} e^{ip(x-y)} \xrightarrow{a \rightarrow 0} \int \frac{dp}{2\pi} \frac{1}{2\omega_p} e^{ip(x-y)}. \quad (6)$$

The two-point function of the scalar defines the scalar mass of the theory. In the continuum limit, when we turn on the interaction  $\lambda_0$ , in the weakly-coupled regime one could compute the correction to the mass through the Feynman diagrams. If the coupling is strong enough, studying the theory becomes challenging with only analytic perturbative techniques. The theory will experience a second-order phase transition at the strong coupling, where the universal behavior belongs to the 2D Ising universality class. In general, computing the two-point function will tell us the information about the mass of the particle in the lattice discretization. In the Appendix, we address the relation between lattice models and their field theory description, emphasizing the importance of simulating quantum field theories.

### B. Jordan-Lee-Preskill algorithm and extension

In this section, we discuss the Jordan-Lee-Preskill algorithm [6, 7]. The algorithm requires the Hamiltonian of the field theory, say the  $\lambda\phi^4$  theory in the lattice, and the input state data specified by some wave packets.

**Algorithm 1** (Jordan-Lee-Preskill [6, 7]). *The algorithm consists the following smaller steps.*

- *State encoding.* We need to formulate a qubit system in a device with a proper number of qubits. In

the Jordan-Lee-Preskill algorithm, we use the field basis in the coordinate space. The number of required qubits is bounded by the scattering energy we need.

- *Preparing initial states in the free theory.* This could be done by the Kitaev-Webb algorithm in the quantum computer [30]. In the scattering experiment, we need some single-particle wave packet states with given momenta as initial states, which could be prepared from the creation operator acting on the Gaussian vacuum.
- *Adiabatic state preparation towards the interacting theory.* This treatment is to convert the wave packets of single particles in the free theory towards reasonable single-particle wave packets in the interacting theory. To achieve this goal, one could use the adiabatic state preparation to slowly turn on the interaction, which is closely related to the mass gap in the  $\lambda\phi^4$  theory.
- *Time evolution of the Hamiltonian.* The evolution in a universal quantum computer is using the product formula (Lie-Trotter-Suzuki formula). Note that the same trick is also used in the adiabatic state preparation procedure.
- *Measurement.* One could measure quantum observables in the system using quantum algorithms (see discussions in Ref. [6, 7]).

In this work, we discuss how to perform the above analysis in the variational platform. Before a more detailed discussion, we will make a brief summary on the variational realization of the Jordan-Lee-Preskill algorithm.

- *State encoding.* There are many choices of bases for bosonic lattice quantum field theory: coordinate space or momentum space, field basis or harmonic oscillator basis. The choice of bases is depending on the purpose of our simulation and the hardware we are going to use. One of the main advantages of the coordinate space is the locality in the action, which will be ruined when we move to the momentum space. However, the Hamiltonian is still sparse in the momentum space, and the variational algorithms may not be sensitive to the locality at all, since the computation is completely done by introducing variational ansatz. Thus, all four combinations of basis choices could be considered, which might provide different levels of convenience in the ground state, wave packet state construction, and measurement, where we will discuss in more detail in later sections, especially Section III (see other formulations of quantum simulation of quantum field theories in the matrix models, especially in the bosonic form [31–37]).

• Preparing initial states for the scattering problem. Different choices of bases will lead to different methods for state preparation. In the field basis, one could construct the ground state using the Kitaev-Webb algorithm, which unfortunately is not suitable for the near-term. One could also use variational forms to find the ground state as a Gaussian distribution (see a related work [38], and an earlier discussion in [39]). Moreover, the ground state and the single-particle states in the free theory are defined naturally in the harmonic oscillator basis in the momentum space. Even if we switch to the harmonic oscillator basis in the coordinate space, the true vacuum state will be slightly different. We will address the above issue in the later sections, especially in Section IV.

• Time evolution of the scattering states. The real time evolution of the algorithm could be done by the variational algorithm in [12, 13]. During the real time evolution, variational errors might be hard to control especially for the non-perturbative regime and violent scattering processes. Nonetheless, we can track the simulation error during the time evolution, and we can adaptively construct the quantum circuit to achieve the desired accuracy within a polynomial circuit depth [16]. We provide a theoretical framework for the dynamics simulation and make comments on the challenges of the scattering process in Section V.

### III. STATE ENCODING

At the starting point, we wish to encode our Hamiltonian from quantum field theory to a quantum device. Thus, we have to choose some computational bases. This section is devoted to having a detailed review and comparison on different versions of bases (see some similar discussions in the quantum chemistry context [40]).

#### A. The field basis in the coordinate space

One of the simplest considerations is the field basis. For a scalar quantum field theory discretized in a lattice, we could define the state decomposition

$$|\psi\rangle = \int_{-\infty}^{\infty} d\phi_1 \cdots \int_{-\infty}^{\infty} d\phi_N \psi(\phi_1, \dots, \phi_N) |\phi_1, \dots, \phi_N\rangle. \quad (7)$$

Here,  $N$  is the total number of sites. The state decomposition for an arbitrary state  $\psi$  gives the above wavefunction  $\psi(\phi_1, \dots, \phi_N)$ , where  $\phi_x$  could choose from an arbitrary number in  $\mathbb{R}$  in principle. The basis is constructed such that a local field operator  $\phi(x)$  hits on the basis will return the real number as its eigenvalue. This

definition is similar to the coordinate basis in quantum mechanics.

Now, since we are using a quantum computer, we need to truncate the local Hilbert space. The states that we are interested in is truncated as

$$|\psi_{\text{cut}}\rangle = \int_{-\phi_{\text{max}}}^{\phi_{\text{max}}} d\phi_1 \cdots \int_{-\phi_{\text{max}}}^{\phi_{\text{max}}} d\phi_N \psi(\phi_1, \dots, \phi_N) |\phi_1, \dots, \phi_N\rangle. \quad (8)$$

Moreover, we want an increment in discretization such that we don't need to choose variables in a continuous interval. Thus, the total number of qubits we need to encode is  $n_b = \lceil \log_2 (1 + 2\phi_{\text{max}}/\delta_\phi) \rceil$ . Assuming the cut-off error such that the state fidelity satisfies  $|\langle \psi_{\text{cut}} | \psi \rangle| = 1 - \epsilon_{\text{cut}}$ , it is shown in Refs. [6, 7] that there are bounds on  $n_b$  from the scattering energy  $E$ , and we have

$$\begin{aligned} \phi_{\text{max}} &= O\left(\sqrt{\frac{NE}{am_0^2\epsilon_{\text{cut}}}}\right), & \delta_\phi &= O\left(\sqrt{\frac{\epsilon_{\text{cut}}}{aNE}}\right), \\ n_b &= O\left(\log\left(\frac{NE}{m_0\epsilon_{\text{cut}}}\right)\right), \end{aligned} \quad (9)$$

where we demand  $\langle \psi | H | \psi \rangle \leq E$ . The bound is derived from the Chebyshev inequality relating the probability outside the range of the field variable cutoff to the field fluctuations, which are bounded by energy based on the expression of the Hamiltonian. The bound is useful to prove the polynomial complexity of the Jordan-Lee-Preskill algorithm, but one should note that the bound itself may not be tight in the practical calculations.

## B. The harmonic oscillator basis in the coordinate space

There is another important basis, the harmonic oscillator basis to define a digital representation of states in lattice quantum field theories. Since we are dealing with a bosonic field theory, the local degrees of freedom are given by harmonic oscillators.

We firstly consider the following transformation,

$$\begin{aligned} \phi(x) &= \frac{1}{(2m_x)^{1/2}} (a_x + a_x^\dagger), \\ \pi(x) &= -i\left(\frac{m_x}{2}\right)^{1/2} (a_x - a_x^\dagger). \end{aligned} \quad (10)$$

Here  $m_x$  is a free parameter we could choose. Then the canonical algebra of  $\phi$  and  $\pi$  leads to the commutation relation  $[a_x, a_y^\dagger] = a^{-1}\delta_{x,y}$ .

Now, the creation operator  $a_x^\dagger$  and its conjugate could define the number states at the site  $x$ . Thus, in the harmonic oscillator basis, we could define the state decom-

position

$$|\psi\rangle = \sum_{n_1=0}^{\infty} \cdots \sum_{n_N=0}^{\infty} \psi(n_1, n_2, \dots, n_N) |n_1, n_2, \dots, n_N\rangle. \quad (11)$$

Here, the number states  $n_x$  are given by creation operators hitting on the vacua for the location  $x$ . Let's say that we are mostly interested in the maximal energy level  $n_{\text{cut}}$ , so we could instead cut the Hilbert space and define

$$|\psi_{\text{cut}}\rangle = \sum_{n_1=0}^{n_{\text{cut}}} \cdots \sum_{n_N=0}^{n_{\text{cut}}} \psi(n_1, n_2, \dots, n_N) |n_1, n_2, \dots, n_N\rangle. \quad (12)$$

## C. The field basis in the momentum space

Now we introduce a basis that is dual to the field basis: the field basis in the momentum space. Remember that we define the dual lattice  $\Gamma$  based on the real lattice  $\Omega$ . Thus, one could directly write the Hamiltonian in terms of the momentum coordinate. To be more specific, consider the free theory solution

$$\begin{aligned} \phi(t, x) &= \int \frac{dk}{(2\pi)\sqrt{2\omega_k}} (a_k + a_{-k}^\dagger) e^{-i\omega_k t + ikx} \\ &\equiv \int \frac{dk}{2\pi} \phi_k(t) e^{ikx}, \end{aligned} \quad (13)$$

with the lattice version

$$\begin{aligned} \phi(t, x) &= \frac{1}{L} \sum_{k \in \Gamma} \frac{1}{\sqrt{2\omega_k}} (a_k + a_{-k}^\dagger) e^{-i\omega(k)t + ikx} \\ &\equiv \frac{1}{L} \sum_{k \in \Gamma} \phi_k(t) e^{ikx}. \end{aligned} \quad (14)$$

We could write the system in terms of the modes  $\phi_k$ . The free theory part is given by

$$\begin{aligned} L_0 &= \int \frac{dk}{(2\pi)} \left[ \frac{1}{2} (\partial_t \phi_k)(\partial_t \phi_{-k}) - \frac{1}{2} \omega_k^2 \phi_k \phi_{-k} \right], \\ H_0 &= \int \frac{dk}{(2\pi)} \left[ \frac{1}{2} \pi_k \pi_{-k} + \frac{1}{2} \omega_k^2 \phi_k \phi_{-k} \right], \end{aligned} \quad (15)$$

and in the lattice we have,

$$\begin{aligned} L_0 &= \frac{1}{L} \sum_{k \in \Gamma} \left[ \frac{1}{2} (\partial_t \phi_k)(\partial_t \phi_{-k}) - \frac{1}{2} \omega(k)^2 \phi_k \phi_{-k} \right], \\ H_0 &= \frac{1}{L} \sum_{k \in \Gamma} \left[ \frac{1}{2} \pi_k \pi_{-k} + \frac{1}{2} \omega(k)^2 \phi_k \phi_{-k} \right], \end{aligned} \quad (16)$$

where we similarly define  $\pi_k = \partial_t \phi_k$ . Now the commutation relation is

$$\begin{aligned} \text{discrete: } & [\phi_k(t), \pi_p(t)] = iL\delta_{k,-p}, \\ \text{continuum: } & [\phi_k(t), \pi_p(t)] = 2\pi i\delta(k+p), \end{aligned}$$

in the continuum. We could also write the interaction piece of the Hamiltonian in the momentum space by

$$\begin{aligned} \text{discrete: } & \frac{\lambda_0}{4!} \sum_{x \in \Omega} \phi^4 = \\ & \frac{\lambda_0}{4!} \frac{1}{L^3} \sum_{k_1, k_2, k_3 \in \Gamma} \phi_{k_1} \phi_{k_2} \phi_{k_3} \phi_{-k_1 - k_2 - k_3}, \\ \text{continuum: } & \frac{\lambda_0}{4!} \int dx \phi^4 = \\ & \frac{\lambda_0}{4!} \int \frac{dk_1 dk_2 dk_3}{(2\pi)^3} \phi_{k_1} \phi_{k_2} \phi_{k_3} \phi_{-k_1 - k_2 - k_3}. \end{aligned} \quad (17)$$

Thus, we could encode the system in the following basis

$$|\psi\rangle = \int \prod_{p_i \in \Gamma} d\phi_{p_i} \psi(\phi_{p_1}, \phi_{p_2}, \dots) |\phi_{p_1}, \phi_{p_2}, \dots\rangle, \quad (18)$$

and we could similarly make a truncation on the field range in the momentum space.

#### D. The harmonic oscillator basis in the momentum space

Similarly, we could consider the harmonic oscillator basis in the momentum space. In this basis, the state decomposition is

$$|\psi\rangle = \sum_{p_i \in \Gamma, n_{p_i} \in [0, n_{\text{cut}}]} \psi(n_{p_1}, n_{p_2}, \dots) |n_{p_1}, n_{p_2}, \dots\rangle. \quad (19)$$

The number states now is generated by the creation operator specified by

$$\phi_k = \frac{1}{\sqrt{2\omega_k}} (a_k + a_{-k}^\dagger), \quad (20)$$

and the dual field momentum. The above state has a very clear physical meaning: the basis directly show the scalar particle numbers in different momenta. This also provides a good initial guess for the excited states in the interacting theory. In Section VI, we discuss the particle excitations in the momentum space in more details.

#### E. A comparison

Comparisons on the various aspects of the encoding schemes need a detailed analysis.

The momentum space is widely used in particle physics. For instance, it is useful to write the Feynman rules and Feynman diagrams in the momentum space. In the momentum space picture, it is also natural to interpret particles as momentum eigenstates in the theory, and the S-matrix should have a clear definition in the momentum space. However, unfortunately, in the momentum space, the Hamiltonians are usually not local,

even if we are studying the free theory. So in order to make the Hamiltonian in a local way, we wish to simulate the Hamiltonian in the coordinate space when we are computing the time evolution dynamics.

The field basis is useful for estimating field correlation functions. For instance, if we wish to read the field distribution for a given state, it is straightforward to use the field basis. However, if we wish to see the state in the space of energies and particle numbers, we might consider using the harmonic oscillator, although those quantities are defined in the sense of the free theory. S-matrix might also have a better interpretation under the harmonic oscillator basis. The paper [39] makes a detailed discussion and numerical comparison between those two bases.

Here, we will give a summary of the number of terms in the Hamiltonian for each basis.

- The field basis in the coordinate space. If we only count the number of terms evaluated purely in the field and field momentum operators, the total number of terms is  $O(N)$ .
- The harmonic oscillator basis in the coordinate space. As we have described before, we will replace the field and field momentum operators in the position space by introducing local harmonic oscillators as the computational basis. Since this happens completely in the position space, the number of total terms in the Hamiltonian is  $O(N)$ , where each local term is made by local creation and annihilation operators and their nearest neighbour products.
- The field basis in the momentum space. As we have discussed before, the Hamiltonian in the momentum space is written in the non-local form. For the free theory Hamiltonian, the number of terms will scale as  $O(N)$  when we count the field and field momentum operators. When we add  $\lambda\phi^4$  interactions, the number of terms will scale as  $O(N^3)$ .
- The harmonic oscillator basis in the momentum space. Similarly, we get  $O(N)$  terms in the free theory, and  $O(N^3)$  terms in the interacting theory.

Moreover, the problem of choosing the basis is closely related to the initial state construction before scattering. Going back to the Jordan-Lee-Preskill situation, in the field basis, the ground state is Gaussian for the free theory, so we could construct the Gaussian state with the help of the Kitaev-Webb algorithm as mentioned before. Then, adiabatic state preparation is used to simulate the single-particle wave packet in the interacting theory. Note that the wave packets centered at a given momentum are in fact *defined* by the above way.

Back to the harmonic oscillator basis, it will be very convenient to work in the momentum space, since the momentum sectors are naturally defined in the free theory by the harmonic oscillator. The basis is also useful to keep track of the simulation results in real-time, since

one could quickly identify the basis overlap and find the particle number and their momenta. For the interacting theory, when the interaction is turned on, one could specify the momentum sectors again by the adiabatic state preparation, and we could use this method to *define* the wave packets in the given momentum sectors.

In summary, one of the main advantages of the momentum space, especially for the harmonic oscillator basis, is to quickly identify the momenta and the particle number of output states during the simulation. Thus, in this paper, we will mainly work on the harmonic oscillator basis in the variational setup.

## IV. VARIATIONAL STATE PREPARATION

### A. The variational ansatz

Variational quantum simulation is a useful technique especially for the near-term quantum computer. The variational algorithm starts by preparing the quantum state by a quantum circuit as

$$|\psi(\theta)\rangle = \left( \prod_{\ell=1}^L U_\ell(\theta_\ell) \right) |\psi_0\rangle. \quad (21)$$

Here  $U_\ell$ s are some unitary operators that could be realized in the quantum device, for instance,  $U_\ell(\theta_\ell) = e^{-i\theta_\ell X_\ell}$ , with the variational parameters  $\theta = (\theta_\ell)$ .  $X_\ell$ s are some Hermitian operators, for instance, elements in the Pauli group, and  $|\psi_0\rangle$  could be some simple initial states that could be easily prepared. The target state will, in principle, be approximated by some optimal choices of  $\theta$ , say  $\theta^*$ , which could be found using the variational principles. For example, a typical problem in quantum simulation is to find the ground state, then we could minimize the energy with respect to the variational parameters  $\langle H \rangle_\theta \equiv \langle \psi(\theta) | H | \psi(\theta) \rangle$ .

The general strategy for the ground state searching is by updating the parameters as

$$\theta_\ell(t+1) = \theta_\ell(t) - \lambda_\ell(t) A^{-1}(\theta(t)) \frac{\partial}{\partial \theta_\ell} \langle H \rangle_{\theta(t)}, \quad (22)$$

where  $\theta_\ell(t)$  represents the optimization dynamics with step  $t$ , and the learning rate is given by  $\lambda_\ell(t)$ . Here, we use  $A(\theta(t))$  to represent the metric matrix at the parameter  $\theta(t)$ . The metric matrix in the gradient descent algorithm is simply the identity matrix. In the following section, we will show its explicit form during the optimization.

The next question is how to choose the initial state  $|\psi_0\rangle$  and  $U_\ell$ s? The precise strategy of choosing  $|\psi_0\rangle$ ,  $U_\ell$  and the optimization scheme will specify the variational quantum algorithm we use. There are many variational algorithms (see Ref. [14, 15] for a recent review). In this work we will discuss the following bosonic unitary coupled cluster (UCC) ansatz and imaginary time evolution where we practically find the best in our physical system.

Different from the quantum computational chemistry literature, where the UCC ansatz consists of the fermionic excitations in the active space, our algorithm expresses the UCC ansatz directly with the bosonic mode.

### B. Bosonic UCC ansatz

As is mentioned before, the variational algorithm may not be very sensitive to the locality of the Hamiltonian. Thus we will focus on the harmonic oscillator basis in the momentum space.

For a single harmonic oscillator,  $h = \omega a^\dagger a$ , the space of the truncated eigenstates  $|s\rangle$  with  $n_{\text{cut}} + 1$  energy levels can be encoded by a compact mapping using  $O(\log n_{\text{cut}})$  qubits. The creation operator and annihilation operator can be represented as

$$a^\dagger = \sum_{s=0}^{n_{\text{cut}}-1} \sqrt{s+1} |s+1\rangle \langle s|, \quad a = \sum_{s=1}^{n_{\text{cut}}} \sqrt{s} |s-1\rangle \langle s|. \quad (23)$$

The ladder operators can be decomposed into Pauli operators with  $O(n_{\text{cut}}^2)$  terms. Thus, we can encode the Hamiltonian with a quantum computer [41]. Prior work has extensively investigated the coupled cluster methods to solve the electronic energy spectra and vibrational structure in the chemistry and materials science, and the quantum version, unitary coupled cluster ansatz, has been suggested and further experimentally demonstrated to solve the chemistry problems on a quantum computer [21, 22]. Other prior works [20, 42] discussed the usage of bosonic UCC in studying vibronic properties of molecules.

The general form of unitary coupled cluster is given by

$$|\psi(\theta)\rangle = \exp\left(\hat{T} - \hat{T}^\dagger\right) |\psi_0\rangle, \quad (24)$$

where  $\hat{T}$  is the sum of symmetry preserved excitation operators truncated at finite excitations as  $\hat{T} = \hat{T}_1 + \hat{T}_2 + \dots$ . The key ingredient of UCC ansatz is to search for the true ground state of the interacting fermionic theory by considering the particle-conserving excitations above a reference state.

In our quantum field theory setup, a bosonic version of the UCC ansatz [20, 42] could be natural to capture types and particle numbers for scalar particles. In the coordinate space, the single and double excitation operators preserving the excitation mode can be expressed as

$$\begin{aligned} \hat{T}_1 &= \sum_{l=1}^L \sum_{s,t=0}^{n_{\text{cut}}} \theta_{s^{(l)}, t^{(l)}} |s^{(l)}\rangle \langle t^{(l)}|, \\ \hat{T}_2 &= \sum_{l_1, l_2} \sum_{s_1, s_2, t_1, t_2=0}^{n_{\text{cut}}} \theta_{s_1^{(l_1)}, t_1^{(l_1)}, s_2^{(l_2)}, t_2^{(l_2)}} |s_1^{(l_1)} s_2^{(l_2)}\rangle \langle t_1^{(l_1)} t_2^{(l_2)}|, \end{aligned} \quad (25)$$

where  $l_1, l_2$  in the superscript denote the site in the coordinate space, i.e. the mode of the harmonic oscillator basis,  $s^{(l)}$  and  $t^{(l)}$  denote the energy level of the  $l$ th site, and  $\theta$  is the variational parameter in terms of certain energy level and site. Here,  $|s^{(l)}\rangle$  and  $\langle t^{(l)}|$  represent the creation and annihilation of the particle excitation carrying energy  $s$  and  $t$  in the  $l$ th harmonic oscillator mode, respectively. The  $\lambda\phi^4$  field could lift the excitation up to 4 levels at each mode so we could constrain the energy level as  $|s_i - t_i| \leq 4$ . Moreover, since we are interested in the low-energy eigenstates, the excitations to high energy levels can be truncated to  $d_1$  and  $d_2$  by considering the dominant low-energy excitations. We note that this ansatz is especially useful for lattice model with strong static correlations. For relatively small  $\lambda_0$ , the discretized  $\lambda\phi^4$  theory in the coordinate space have strong locality. Therefore, we expect this ansatz would be suitable for this problem.

In the momentum space, the effective action preserves the momentum reflection symmetry ( $p \rightarrow -p$ ). Therefore, we may express the single and double excitation operators of the bosonic UCC ansatz in the momentum space as

$$\begin{aligned}\hat{T}_1 &= \sum_k \sum_{s,t=0}^{n_{\text{cut}}} \theta_{s^{(k)},t^{(k)}} |s^{(k)}\rangle \langle t^{(k)}|, \\ \hat{T}_2 &= \sum_{k_1,k_2} \sum_{s_1,s_2,t_1,t_2=0}^{n_{\text{cut}}} \theta_{s_1^{(k_1)},t_1^{(k_1)},s_2^{(k_2)},t_2^{(k_2)}} \times \\ &\quad \left( |s_1^{(k_1)} s_2^{(k_2)}\rangle \langle t_1^{(k_1)} t_2^{(k_2)}| + |s_1^{(\tilde{k}_1)} s_2^{(\tilde{k}_2)}\rangle \langle t_1^{(\tilde{k}_1)} t_2^{(\tilde{k}_2)}| \right).\end{aligned}\quad (26)$$

Here, we use the same notation as in Eq. (25) and  $k$  ( $\tilde{k} = -k$ ) is the (reversed) momentum. We can similarly have the constraint  $|s_i - t_i| \leq 4$  for the  $\lambda\phi^4$  field in the momentum space.

This type of ansatz could be useful for the  $\lambda\phi^4$  quantum field theory since the four-point coupling could induce the  $2 \rightarrow 2$  scattering process, which represents two excitations coming in and two excitations moving out in the perturbation theory and the Feynman diagram (note that this argument is relatively heuristic, since the expansion from the exponential will induce more complicated terms).

Other heuristic ansatz that takes account of the symmetries of the  $\phi^4$  field could be designed. For instance, one may construct the ansatz in the momentum space as

$$\hat{T}_1 = \sum_k \sum_{s,t=0}^{n_{\text{cut}}} \theta_{s^{(k)},t^{(k)}} |s^{(k)}\rangle \langle t^{(k)}|, \quad (27)$$

$$\begin{aligned}\hat{T}_2 &= \sum_k \sum_{s_1,s_2,t_1,t_2=0}^{n_{\text{cut}}} \theta_{s_1^{(k)},t_1^{(k)},s_2^{(\tilde{k})},t_2^{(\tilde{k})}} \times \\ &\quad \left( |s_1^{(k)} s_2^{(\tilde{k})}\rangle \langle t_1^{(k)} t_2^{(\tilde{k})}| + |s_1^{(\tilde{k})} s_2^{(k)}\rangle \langle t_1^{(\tilde{k})} t_2^{(k)}| \right),\end{aligned}\quad (28)$$

which considers the pairing correlations of the momentum  $k$  and  $\tilde{k}$ . Compared to ansatz in Eq. (26), this ansatz

reduces a large number of parameters in the ansatz, and could be efficient for the implementation and optimization in practice. We may even discard the second term in Eq. (28) to further reduce the gate count in the variational quantum circuits. Especially, we find this ansatz works well numerically.

Now, say that we can decompose the operator  $\hat{T}$  into Pauli operators as  $\hat{T} = \sum_j \alpha_j \hat{P}_j$ , with elements of the Pauli group  $\hat{P}_j \in \{I, \sigma_x, \sigma_y, \sigma_z\}^{\otimes n}$ , and the variational parameters  $\alpha_j$ . Then the unitary coupled cluster operator can be decomposed in terms of the imaginary part of  $\hat{T}$  as  $\exp(\hat{T} - \hat{T}^\dagger) = i \sum_{j'} \alpha_{j'} \hat{P}_{j'}$ . We can use the first-order Trotter formula,  $\exp(\hat{T} - \hat{T}^\dagger) \approx \prod_{j'} \exp(i \alpha_{j'} \hat{P}_{j'})$ , where each term can be efficiently implemented on a quantum computer. It is worth mentioning that since the ansatz in Eq. (25) and Eq. (26) is local in terms of the mode, and therefore the Pauli terms could be easily calculated.

### C. Variational quantum algorithms

We now discuss how to use variational quantum algorithms for finding the ground state and the low-lying excited states. We first briefly review the variational quantum simulation algorithm of imaginary time evolution [19]. The normalized imaginary time evolution at imaginary time  $\tau$  is given by  $|\psi(\tau)\rangle = \frac{e^{-H\tau}|\psi_0\rangle}{\sqrt{\langle\psi_0|e^{-2H\tau}|\psi_0\rangle}}$ . The population of the energy eigenstate  $|e_j\rangle$  will decay exponentially with the energy  $E_j$ , and the ground state can be obtained in the long time limit  $|\psi^{(0)}\rangle = \lim_{\tau \rightarrow \infty} |\psi(\tau)\rangle$ . While the nonunitary imaginary time evolution cannot be directly implemented on a quantum computer, one could still simulate imaginary time evolution on a quantum computer by using the hybrid quantum-classical algorithm. Instead of simulating the imaginary time evolution directly, we assume that the time-evolved state can be approximated by a parametrized trial state  $|\psi(\theta(\tau))\rangle$ , with variational parameters  $\theta(\tau) = (\theta_\mu(\tau))$ . As mentioned in [19], by minimizing the distance between the ideal evolution and the evolution of the parametrized trial state, the evolution of the target state  $|\psi(\tau)\rangle$  under the Schrödinger equation can be mapped to the trial state manifold as the evolution of parameters  $\theta$ .

Using McLachlan's variational principle, we have

$$\delta \|(d_\tau + H - E_\tau) |\psi(\theta(\tau))\rangle\| = 0, \quad (29)$$

and the evolution of the parameters under the imaginary time evolution could be determined by

$$\sum_j A_{i,j} \dot{\theta}_j = -C_i, \quad (30)$$

with the matrix elements of  $A$  and  $C$  given by

$$\begin{aligned} A_{i,j} &= \text{Re}(\partial_i \langle \psi(\theta(\tau)) | \partial_j | \psi(\theta(\tau)) \rangle), \\ C_i &= \text{Re}(\partial_i \langle \psi(\theta(\tau)) | H | \psi(\theta(\tau)) \rangle). \end{aligned} \quad (31)$$

Here,  $\| |\psi\rangle \| = \sqrt{\langle \psi | \psi \rangle}$  is the norm of the quantum state, we denote  $\partial_i \equiv \partial / \partial \theta_i$ , and we assume the parameters are real. By tracking the evolution of the variational parameters, we can effectively simulate imaginary time evolution. This actually serves as an optimizer to update the parameters in Eq. (22). It is worth mentioning for the pure state imaginary time evolution, this approach is equivalently to the quantum natural gradient descent method, and the matrix  $A$  is indeed the Fisher matrix [43].

Moreover, having found the ground state  $|\psi^{(0)}\rangle$ , we can construct a modified Hamiltonian  $H^{(1)} = H + \alpha |\psi^{(0)}\rangle \langle \psi^{(0)}|$ , where  $\alpha$  is the regularization term that lifts the ground state energy, and is sufficiently large comparing to the energy scale of the system.

The ground state of the modified Hamiltonian  $H^{(1)}$  becomes  $|\psi^{(1)}\rangle$ , the first excited state  $|\psi^{(1)}\rangle$  of the original Hamiltonian  $H$ . As  $|\psi^{(0)}\rangle$  is an excited state of the modified Hamiltonian, we can evolve the system under  $H^{(1)}$  in the imaginary time to suppress the spectral weight of  $|\psi^{(0)}\rangle$  and obtain the first excited state  $|\psi^{(1)}\rangle$ . This process can be repeated to obtain the higher-order excited states. More specifically, the  $(n+1)$ th excited state is the ground state of effective Hamiltonian

$$H^{(n+1)} = H + \alpha \sum_{j=0}^n |\psi^{(j)}\rangle \langle \psi^{(j)}|. \quad (32)$$

Instead of preparing the Hamiltonian directly, we can simulate the imaginary time evolution under  $H^{(n+1)}$  by tracking the evolution of the parameters, which are now modified as

$$\begin{aligned} C_i &= \text{Re}(\partial_i \langle \psi(\theta(\tau)) | H | \psi(\theta(\tau)) \rangle + \\ &\quad \alpha \sum_{j=0}^n \partial_i \langle \psi(\theta(\tau)) | \psi^{(j)} \rangle \langle \psi^{(j)} | \psi(\theta(\tau)) \rangle), \end{aligned} \quad (33)$$

while the matrix  $A$  keeps the same as in Equation (31). These addition terms in  $C_i$  can be evaluated using the low-depth swap test circuit. Other variational excited state preparation techniques can be found in a recent review paper [14].

We wish to remark that the circuit ansatz for the imaginary time evolution does not have to be fixed. Instead, the circuit ansatz could be adaptively determined by tracking the distance of the ideal evolved state and the variational state. In the extreme case, we could construct the circuit by approximating the normalized state at every single time step, which reduces to the quantum imaginary time evolution, firstly proposed in Ref. [44]. Suppose the Hamiltonian has the decomposition  $H = \sum_{l=1}^L \hat{h}_l$ , where the Hamiltonian contains  $L$

local terms and each  $\hat{h}_l$  acts on at most  $k$  neighboring qubits. Using the first-order Trotterization, the evolved state after applying nonunitary operator  $e^{-\delta\tau\hat{h}_l}$  within imaginary time  $\delta\tau$  by

$$|\Psi(\tau + \delta\tau)\rangle = c^{-1/2} e^{-\delta\tau\hat{h}_l} |\Psi(\tau)\rangle \approx e^{-i\delta\tau\hat{A}} |\Psi(\tau)\rangle, \quad (34)$$

where  $c$  is the normalization factor and  $\hat{A}$  is a Hermitian operator that acts on a domain of  $D$  qubits around the support of  $\hat{h}_l$ . The unitary operator  $e^{-i\delta\tau\hat{A}}$  can be determined by minimizing the approximation error in Eq. (34), which is similar to the derivation in Eq. (29). For a nearest-neighbor local Hamiltonian on a  $d$ -dimensional cubic lattice, the domain size  $D$  is bounded by  $\mathcal{O}(C^d)$ , where  $C$  is the correlation length. More details about the algorithm complexity can be found in Ref. [44].

This circuit construction strategy can be regarded as a special case in the variational imaginary time evolution given by Eq. (29) and Eq. (31). If we fix the old circuit ansatz  $\theta(\tau)$  constructed before imaginary time  $\tau$ , and determine the new added unitary operator  $\theta(\delta\tau)$  that approximates the effect of  $e^{-iH\delta\tau}$ , this is exactly the same as Eq. (34). However, to further reduce the circuit depth, we can jointly optimize the parameters  $\theta(\tau) \oplus \theta(\delta\tau)$ , making it more compatible for the near-term quantum devices.

#### D. Spectral crowding

Before we start to apply variational algorithms, we will make a short investigation on the spectrum of the  $\lambda\phi^4$  quantum field theory. In the momentum space, harmonic oscillator basis, one might have a large number of degeneracies in the energy eigenstates (similar problems appear in other bases as well), bringing potential problems for quantum simulation. We will borrow the terminology ‘‘spectral crowding’’ that has been used in the ion trap systems [45] referring to this situation.

For excited states, degeneracy might happen even in the free theory in our construction. For instance, say that in the free theory, it might be the case where

$$\sum_i n_i \omega(p_i) = \sum_j \bar{n}_j \omega(\bar{p}_j). \quad (35)$$

Here, we have states represented in the harmonic oscillator basis in the momentum space, with particle numbers and momenta  $n_i, p_i$ , or  $\bar{n}_j, \bar{p}_j$ , and their energies are precisely identical. A typical example is that considering the continuum limit, we might have

$$n |m_0| = \sqrt{m_0^2 + p^2}, \quad (36)$$

where  $n \in \mathbb{Z}_{>0}$ . In those cases, their states are degenerate. Another typical case the role of parity which anti-commutes with the momentum:

$$\omega(p) = \omega(-p), \quad (37)$$

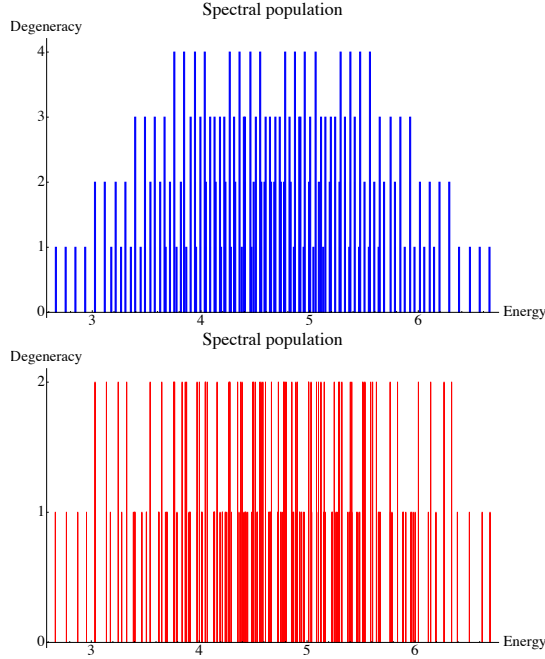


FIG. 1. Spectral crowding for  $\lambda\phi^4$  theory: Blue/left: free theory; Red/right: interacting theory. We use  $m_0 = 0.369$  and  $\lambda_0 = 0$  (free) or  $\lambda_0 = 0.481$  (interacting), with maximally three excitations  $n_{\text{cut}} = 3$ , system size  $N = 4$ , and the lattice spacing  $a = 1$ , for the harmonic oscillator basis in the momentum space.

since we are not able to distinguish the left-moving and right-moving states only by their energies. Figure 1 provides an example for spectral crowding, where we fix  $m_0 = 0.369$  and  $\lambda_0 = 0$  (free) or  $\lambda_0 = 0.481$  (interacting), with maximally three excitations  $n_{\text{cut}} = 3$ , system size  $N = 4$ , and the lattice spacing  $a = 1$ . The choice of parameters is aiming on avoiding the situation in the Eq. (36).

Spectral crowding might bring us difficulties on identifying states in the output, and defining different directions of momenta for particles, especially when states are excited. Instead of looking at the general structure of density of states, we start with the maximally one-particle states in this simple system. In the free theory, we have the ground state with the energy 2.662. Moreover, the single-particle states have the energies:

$$p = \frac{2\pi}{L}(0, 1, 2, 3) : E = 2.754, 3.027, 3.170, 3.027. \quad (38)$$

We know that this degeneracy is made by the boundary condition of the momentum  $p \sim 2\pi/L - p$ , which is the parity  $\mathbb{Z}_2$  [46]. In general, for an  $n$ -particle state, since we could freely choose the direction of momentum, the spectral crowding will be enhanced at least  $O(2^n)$ .

Now, we consider to turn on the interaction. In the adiabatic process where we slowly turn on the  $\phi^4$  Hamiltonian,

$$H(s) = H_0 + s\lambda_0 H_I, \quad (39)$$

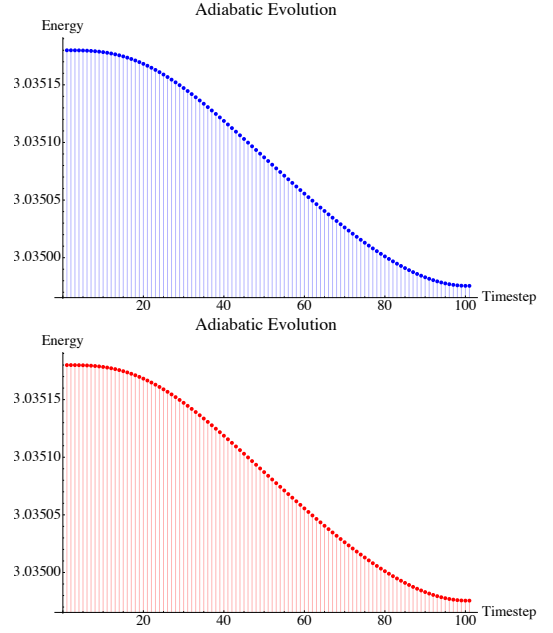


FIG. 2. Adiabatic evolution starting from the free particle momenta  $p = \frac{2\pi}{L}(1, 3)$  (left/blue,right/red). Those two examples have the adiabatic errors both around 0.07%.

and  $s \in [0, 1]$ , since the interacting Hamiltonian is invariant under the parity transformation, we could use the adiabatic process to *define* the direction of the momentum. In Figure 2, we show an example of the adiabatic evolution numerically, with the number of adiabatic steps  $T = 100$  (which means that we are dividing the interval  $s \in [0, 1]$  to 101 steps). We find all single-particle eigenstates could agree with the corresponding energy eigenstates with high fidelities (we only show  $p = \frac{2\pi}{L}(1, 3)$  example in the plot, but all four adiabatic state preparations are also verified). Note that this operation specifies the direction of momenta in the interacting theory. This is an advantage of our basis, where we could specify the direction of momenta in this way.

The above algorithm could also be made variationally. Recall that in the variational process, we are starting from a wave packet state  $|\psi\rangle_{\text{initial}}$ , and we slowly turn on the interaction  $\lambda$  from the free theory  $\lambda = 0$ . Thus, during this process, the Hamiltonian is time-dependent. Instead of considering Lie-Trotter-Suzuki decomposition in a digital quantum computer, one could perform the above calculation in a quantum computer with a variational form. We will use the variational approach of time evolution introduced in Refs. [13, 19]. Similar to the imaginary time proposal, we will use the McLachlan's variational principle and take care of the time-dependent global phase.

Now consider the situation where we adiabatically turn on the coupling of the Hamiltonian. We restrict our so-

lution inside the variational form similar from before,

$$|\psi(\theta)\rangle = \left( \prod_{\ell=1}^L U_\ell(\theta_\ell) \right) |\psi_{\text{free theory states}}\rangle. \quad (40)$$

Note that we are starting from the corresponding momentum eigenstates of the free particle. The differential equation of  $\theta$  based on the McLachlan's variational principle is given by

$$\sum_j M_{i,j} \frac{d\theta_j}{ds} = V_i, \quad (41)$$

where

$M_{i,j} = \text{Re}A_{i,j} + \partial_i\langle\psi(\theta(s))|\psi(\theta(s))\rangle\partial_j\langle\psi(\theta(s))|\psi(\theta(s))\rangle$ ,  $V_i = \text{Im}C_i + i\partial_i\langle\psi(\theta(s))|\psi(\theta(s))\rangle\langle\psi(\theta(s))|H(s)|\psi(\theta(s))\rangle$ , and  $A$  and  $C$  are similarly defined in Eq. (31). One could show that the solution of  $\theta$ s are always real in our variational form, and the variational answer is consistent with the actual answer up to a time-dependent global phase. More detailed discussions on the simulation error during the dynamics can be found in Section V.

Similar to the above variational adiabatic state preparation algorithm, the imaginary time evolution could also start from the corresponding free theory states. Practically, we find in our example, the imaginary time evolution algorithm performs better (this is intuitively because we are looking for low-lying states with low energies).

Moreover, these methods can be integrated together. We can turn on the interaction, similarly as in Eq. (39), but with much fewer steps. We could then use the variational algorithms to find the ground state of the intermediate Hamiltonian  $H(s)$ , using which as the initial state for the next time step until  $s$  reaches 1. Compared to finding the ground state of  $H_I$ , this method may avoid the local minimum.

Finally, we comment on other methods to snake around the spectral crowding problem. A useful trick to find the state with both fixed momentum and energy is through measurement in quantum devices. We could consider measuring the momentum operator

$$P = a \sum_{x \in \Omega} \pi \nabla_a \phi, \quad (42)$$

during the variational process, making sure that it keeps the sign when the interaction is turning on. However, the momentum operator only has its meaning in the free theory, so we only expect the above algorithm to be useful in the sense of weakly-coupled theory.

Another useful trick for keeping the momentum is similar to the idea of the tangent space method in the language of matrix product state (see a review [47]). Usually, we expect that our momentum- $p$  eigenstate could have the following form

$$|\Phi_p\rangle = \sum_{x \in \Omega} e^{ipx} T_x |\Phi\rangle. \quad (43)$$

Here  $T_x$  is the translation operator with the vector  $x$ . If the state  $|\Phi\rangle$  is already a momentum- $p$  eigenstate,

$$|\Phi\rangle = \sum_{y \in \Omega} e^{ipy} T_y |\Psi\rangle, \quad (44)$$

we have

$$\begin{aligned} \sum_{x \in \Omega} e^{ipx} T_x \sum_{y \in \Omega} e^{ipy} T_y |\Psi\rangle &= \sum_{x,y \in \Omega} e^{ip(x+y)} T_{x+y} |\Psi\rangle \\ &= \sum_{x,z \in \Omega} e^{ipz} T_z |\Psi\rangle \propto \sum_{z \in \Omega} e^{ipz} T_z |\Psi\rangle. \end{aligned} \quad (45)$$

Moreover, if the state  $|\Phi\rangle$  is a linear superposition of the momentum- $p$  state and the momentum- $(-p)$  state where  $p \neq 0$

$$\begin{aligned} \sum_{x \in \Omega} e^{ipx} T_x \left( c_1 \sum_{y \in \Omega} e^{ipy} T_y |\Psi\rangle + c_2 \sum_{y \in \Omega} e^{-ipy} T_y |\Psi\rangle \right) \\ = \# \times c_1 \sum_{z \in \Omega} e^{ipz} T_z |\Psi\rangle + c_2 \sum_{x,y \in \Omega} e^{ip(x-y)} T_{x+y} |\Psi\rangle \\ = \# \times c_1 \sum_{z \in \Omega} e^{ipz} T_z |\Psi\rangle + c_2 \sum_u e^{ipu} \sum_v T_v |\Psi\rangle \\ \sim \# \times c_1 \sum_{z \in \Omega} e^{ipz} T_z |\Psi\rangle. \end{aligned} \quad (46)$$

Note that the  $c_2$  term is suppressed because it sums over a pure numerical phase. Thus, for the state we obtained from the variational quantum simulation, we could make a linear superposition weighted by  $e^{ipx}$  to obtain a momentum eigenstate with a fixed momentum direction, at least in the case of the single-particle scattering experiment. However, the above method seems to be mostly useful when we know how to construct the translation operator. It is manifest in the coordinate space, but not easy in the momentum space.

## E. One-particle subspace fidelity and generalizations

Here we discuss some concepts about fidelities that are useful for the variational, scattering-state preparation setting. Say that we originally have a wave packet centered around a given momentum, and it is a one-particle state in the free theory. Now we could turn on the interaction slowly. Ideally, as we discussed before, a one-particle state will still remain a one-particle state in the interacting theory. In fact, if we consider momentum eigenstates of a single particle,  $|p\rangle$ , we could define the one-particle subspace by

$$V_{\text{one-particle,free}} = \text{span}_p(|p\rangle). \quad (47)$$

Now, if we are adiabatically turning on each state  $|p\rangle$  towards the coupling  $\lambda_0$ , the space will become

$$V_{\text{one-particle},\lambda_0} = \text{span}_p(\text{adiabatic evolution}_{\lambda_0} \circ |p\rangle). \quad (48)$$

In fact, if the adiabatic evolution is slow enough, the above expression will define the one-particle space in the interacting theory. This makes our momentum eigenstate definition more precise.

Now, say that we are doing the state preparation using the variational algorithm (which is not the ideal adiabatic process). Due to the limitation induced by the variational ansatz, we will have some systematic errors (or other errors). However, the resulting state, although suffering from the noise, might still have a large overlap with the one-particle subspace  $V_{\text{one-particle}, \lambda_0}$ . In fact, we could define the state fidelity

$$F_{\text{state,adiabatic}} = |\langle \psi_{\text{ideal}} | \psi_{\text{variational}} \rangle|, \quad (49)$$

which is an overlap between the accurate state from an ideal adiabatic simulation without any error, and the state obtained from the variational algorithm. We could also define the one-particle subspace fidelity

$$F_{\text{one-particle,adiabatic}} = |\langle \psi_{\text{variational}} | \Lambda | \psi_{\text{variational}} \rangle|. \quad (50)$$

Here,  $\Lambda$  is the projector of the space  $V_{\text{one-particle}, \lambda_0}$ . By definition, if  $F_{\text{state,adiabatic}}$  is high enough,  $F_{\text{one-particle,adiabatic}}$  should also be high enough.

In principle, we wish our fidelities to be always high enough, which means that we are performing high-quality state preparations. Ideally, we wish the state fidelity to be high. But in practice, when we do not really care about the form of the wave packet, and we only care about if the state is still approximately a one-particle state, we could only use the one-particle subspace fidelity. As a summary, the level of requirements we want about fidelities is closely related to the actual physical motivation we have in the simulation experiment. A successful benchmark for our variational algorithm about the adiabatic state preparation before particle scattering will require a detailed check about fidelities in a lower number of clean qubits before scaling the system up.

Let us end this subsection by making a final comment on the fidelities. The definition of fidelities is indeed related to the physical task we want when doing the experiment. The definition of one-particle subspace fidelity corresponds to the choice when we wish to maintain the one-particle subspace during the initial state preparation. When we have other requirements, we could demand other versions of fidelities be high. For instance, we could define the momentum fidelity by measuring the momentum center of the wave packet. We could also define the wave packet profile fidelity by measuring the wave packet form. Stronger definitions on fidelities would require higher quality when we are doing the variational state preparation.

In the most general setting, we could define the projector to the subspace  $\Lambda$  as

$$\Lambda = \sum_{i=1}^{D_\Lambda} |q_i\rangle \langle q_i|, \quad (51)$$

where  $|q_i\rangle$  is the basis and  $D_\Lambda$  is the dimension of the subspace. Thus, for a variational state  $|\psi\rangle$  we have

$$\begin{aligned} |\psi\rangle &= \sum_{i=1}^{D_\Lambda} c_i |q_i\rangle + c_e |e\rangle = \Lambda |\psi\rangle + c_e |e\rangle \\ &= \Lambda |\psi\rangle + (1 - \Lambda) |\psi\rangle. \end{aligned} \quad (52)$$

Here  $c_i$  and  $c_e$  are the expansion coefficients, and  $|e\rangle$  is the perpendicular component of the subspace projector  $\Lambda$ . Say that the state is normalized, we have

$$\left( \sum_{i=1}^{D_\Lambda} c_i^* c_i \right) + |c_e|^2 = 1. \quad (53)$$

Thus, the subspace fidelity is defined as

$$F_\Lambda = |\langle \psi | \Lambda | \psi \rangle| = \sum_{i=1}^{D_\Lambda} c_i^* c_i = 1 - |c_e|^2. \quad (54)$$

At the same time, the ideal state is given by the expansion coefficients  $d_i = c_i + \varepsilon_i$ ,  $|\psi_{\text{ideal}}\rangle = \sum_{i=1}^{D_\Lambda} d_i |q_i\rangle$ , and thus the state fidelity is given by

$$\begin{aligned} F_{\text{state}} &= |\langle \psi_{\text{ideal}} | \psi \rangle| = \left| \sum_{i=1}^{D_\Lambda} d_i^* c_i \right| \\ &= \left| \sum_{i=1}^{D_\Lambda} c_i^* c_i + \sum_{i=1}^{D_\Lambda} \varepsilon_i^* c_i \right| = \left| 1 - |c_e|^2 + \sum_{i=1}^{D_\Lambda} \varepsilon_i^* c_i \right| \\ &= \left| F_\Lambda + \sum_{i=1}^{D_\Lambda} \varepsilon_i^* c_i \right|. \end{aligned} \quad (55)$$

This equation illustrates the relation between the state fidelity and the subspace fidelity. In the limit where  $\varepsilon$  are small, those two fidelities are almost equal [48].

## V. PARTICLE SCATTERING

Similar to the variational state preparation, we could also make the variational version of particle scattering. Now, when we are considering the variational time evolution, the only difference comparing to the adiabatic state preparation, is that now the Hamiltonian is static, and the bare coupling  $\lambda_0$  is fixed. The evolution of the variational parameter is given by

$$\sum_j M_{i,j} \frac{d\theta_j}{dt} = V_i \quad (56)$$

where  $M$  and  $V$  can be similarly expressed as

$$\begin{aligned} M_{i,j} &= \text{Re} A_{i,j} + \partial_i \langle \psi(\theta(t)) | \psi(\theta(t)) \rangle \partial_j \langle \psi(\theta(t)) | \psi(\theta(t)) \rangle, \\ V_i &= \text{Im} C_i + i \partial_i \langle \psi(\theta(t)) | \psi(\theta(t)) \rangle \langle \psi(\theta(t)) | H | \psi(\theta(t)) \rangle. \end{aligned}$$

Here the Hamiltonian  $H$  does not depend on the time  $t$ .

Now we show how to approximate the ideal evolved state during the dynamics up to given error  $\varepsilon$ . Suppose at time  $t$  the ideal state  $\Phi(t)$  is approximated by  $\Phi(t) \approx |\Psi(\theta(t))\rangle$ . Within time step  $\delta t$ , we evolved the state  $|\Psi(\theta(t))\rangle$  by updating the parameters  $\theta(t)$  to  $\theta(t + \delta t)$ , which introduces an approximation error at  $t + \delta t$  as

$$\delta\varepsilon = \|\langle \Psi(\theta(t + \delta t)) \rangle - e^{-iH\delta t} |\Psi(\theta(t))\rangle\|. \quad (57)$$

Minimizing the error will give the similar results as that from the McLachlan's variational principle in Eq. (56). In the extreme case, if we choose the unitary operators in the ansatz  $U_\ell$  from all the Hamiltonian terms ( $\hat{h}_l$ ), for instance the Trotterization, this error could be reduced to zero. This indicates that for single step, we can guarantee the simulation error at each time  $t$  up to certain threshold.

We can also track the accumulated error during the whole scattering process. Starting from an initial state  $|\Psi_0\rangle$ , the accumulated error until time  $t + \delta t$  can be bounded by

$$\begin{aligned} \varepsilon &= \|\langle \Psi(\theta(t + \delta t)) \rangle - e^{-iH\delta t} |\Phi(t)\rangle\| \\ &\leq \sum_{\delta t} \|\langle \Psi(\theta(t + \delta t)) \rangle - e^{-iH\delta t} |\Psi(\theta(t))\rangle\| = \sum_{\delta t} \delta\varepsilon, \end{aligned} \quad (58)$$

where we have used triangle inequality and the distance invariance under the unitary transformation in the second line. The single step error can be bounded by

$$\delta\varepsilon = \sqrt{\Delta^2 \delta t^2 + O(\delta t^3)}, \quad (59)$$

where the first-order order error is

$$\Delta^2 = \langle H^2 \rangle + \sum_{jj'} A_{jj'} \dot{\theta}_j \dot{\theta}_{j'} - 2 \sum_j C_j \dot{\theta}_j, \quad (60)$$

with the matrix  $A$  and  $C$  defined in Eq. (31). The total error during the simulation can be bounded by

$$\varepsilon \leq T \max \Delta, \quad (61)$$

where  $\max \Delta$  is the maximum error during the evolution. In practice, we could add the operators from the Hamiltonian term ( $\hat{h}_l$ ) into the circuits to decrease the error to a certain threshold  $\varepsilon_0$  by setting  $\Delta_{\text{cut}} = \varepsilon_0/T$ . Therefore, by tracking the simulation error at each step, we can ensure the simulation accuracy.

If at time  $t$ , the error  $\Delta(t)$  is measured to be above the threshold, i.e.,  $\Delta(t) > \Delta_{\text{cut}}$ , we repeat to add new operators from the Hamiltonian term ( $\hat{h}_l$ ) until  $\Delta \leq \Delta_{\text{cut}}$ . The efficiency of the adaptive strategy is guaranteed by the following theorem.

**Theorem 2** (Theorem 1 in Ref. [16]). .

1. *The first-order error  $\Delta$  strictly decreases at each iteration until 0;*

2. *In each circuit construction process (if  $\Delta(t) > \Delta_{\text{cut}}$ ), each Pauli term,  $\hat{h}_l$ , in the Hamiltonian is only needed to appear once;*
3. *We can achieve an error  $\Delta \leq \Delta_{\text{cut}}$  in at most  $L$  iteration for any  $\Delta_{\text{cut}} \geq 0$ .*

The key idea of the proof is that in the circuit construction subroutine, there always exists an operation  $\hat{h}_k \in (\hat{h}_l)$ , by appending which to the old circuit, the distance strictly decreases if  $\Delta \neq 0$ . Theorem 2 indicates that circuit construction process will terminate in a finite number of steps during the total time evolution. In an extreme case, we can optimize the parameters directly to make  $\Delta \leq \Delta_{\text{cut}}$ , such that no additional gates are required to be added. This reduces to the conventional variational algorithms in Eq. (56).

We also remark that  $\Delta$  is a measurable quantity. The additional measurement cost for the adaptive circuit construction comes from  $\langle H^2 \rangle$ , which could be measured efficiently by using the compatibility of the Pauli operators in the Hamiltonian. For instance, if  $\hat{h}_l$  and  $\hat{h}_k$  qubit-wise commute with each other, we can simultaneously measure them within one Pauli basis, which can significantly reduce the measurement cost.

We conclude this section by making the following comments about the variational realization of the particle scattering algorithm.

- The bosonic ansatz in Eq. (25) in the coordinate space and Eq. (26) in the momentum space allows the creation of new particles during the scattering process, and they could capture the particle excitations along time evolution.
- Since we are considering the scattering process of the wave packet states, some challenges might appear because of the limitation of the variational ansatz: we cannot cover the full space during the variational simulation. Furthermore, besides the error appearing in the near-term quantum devices, we might have some other errors in the variational process due to the level crossing phenomena among different excited states. For a given theory, lots of tests need to be done to obtain some numerically satisfying results, and we leave those opportunities to future research.
- During the scattering process, we might wish to read off some explicit results for the S matrix elements. Thus, the result should be sensitive to the error, from the adiabatic state preparation to the scattering process. In this situation, we don't want uncontrolled errors from the quantum noise or some systematic errors from the assumption of the variational ansatz. However, if we only want some collective, statistical properties of the output states, for instance, some macroscopic quantities or random averages that could contain some intrinsic

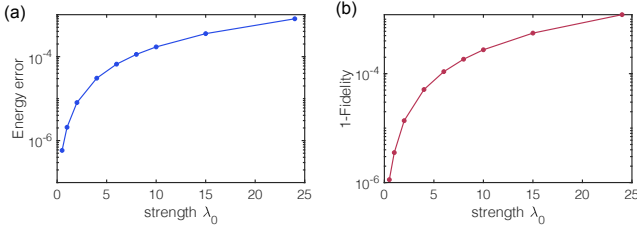


FIG. 3. Variational ground state preparation in the momentum space. The initial state is prepared as  $|0\rangle^{\otimes 8}$  in the computational basis, i.e., the vacuum state of the free Hamiltonian. (a) The error of the ground state energy with an increasing strength of the  $\phi^4$  field  $\lambda_0$ . (b) The fidelity error of the ideal ground state and the variational state with an increasing strength of the  $\phi^4$  field  $\lambda_0$ .

noises (for instance, the jets), we might have fewer constraints on the fidelity of the variational algorithm.

- Other hybrid-classical quantum simulation methods, such as hybrid tensor networks [49], could be leveraged to simulate this scattering process with fewer quantum resources. Moreover, perturbative quantum simulation methods that does not rely on the circuit ansatz could be applied in this task [50].

## VI. NUMERICAL RESULTS

In this section, we demonstrate how the techniques can be used to find the ground state and excited states of the interacting lattice field. We also discuss the spectrum of the lattice field with different bare mass and coupling strength.

Similar to the analysis before, we consider a lattice  $\Omega$  with total length  $L = 4$  and lattice spacing  $a = 1$ , and its dual lattice  $\Gamma$  has 4 sites in the momentum space. We use the harmonic oscillator basis in the momentum space with  $n_{\text{cut}} = 4$  energy levels. To benchmark the performance of the variational algorithms, we consider finding the ground state using the bosonic UCC ansatz with an increasing coupling of the interacting field. We prepare the initial state as the ground state,  $|0\rangle^{\otimes 8}$ , in the free theory. Here, we use the compact mapping for the creation and annihilation operators in Eq. (23). We truncate the highest energy level to be 3 in the double excitation operator in Eq. (28) to reduce the number of parameters and the quantum circuit depth. In order to find the variational state, we use the imaginary time evolution to evolve and identify the low-lying spectra in the interacting theory. The regularization term in the excited state search is fixed as  $\alpha = 8$ . In the numerical simulation, the error of the results is compared with exact diagonalization.

The relative error of the ground state energy and the state associated with different coupling strengths

of the interacting field,  $\lambda_0$ , is shown in Figure 3. We characterize the relative energy error by  $(E_{\text{variational}} - E_{\text{ideal}})/E_{\text{ideal}}$ , where  $E_{\text{ideal}}$  is the corresponding eigenenergies calculated by the exact diagonalization. The state fidelity is defined by the overlap between the variational state and the ideal excited state  $\langle \psi_{\text{ideal}} | \psi_{\text{variational}} \rangle$ . We can see that the simulation error increases when the interaction strength  $\lambda_0$  increases, ranging from  $\lambda_0 = 0.5 \sim 4!$ , but even for a large interaction strength  $\lambda_0 = 4!$ , we can achieve a high simulation accuracy below  $10^{-3}$  both for the energy error and the state fidelity, which indicates a strong representation capability of the quantum circuit ansatz. In the following, we will choose two coupling strength  $\lambda_0 = 1$  and  $\lambda_0 = 10$  to test the performance of the variational algorithms in several regimes [51].

Moreover, we extend the discussions to the excited state preparation, which could be more complicated due to the spectral crowding and degeneracy of the lattice field. We first consider the static mass  $m_0 = 1.27$ , such that the energy of single-particle excitation is lower than that of multi-particle excitations in both the free field and interacting field. In this case, we prepare the initial state for the excited states, searching in the corresponding single-particle excited-state space of the free Hamiltonian  $\lambda_0 = 0$ .

We show the relative error of the energy and the fidelity of the ground state and low-lying excited states towards the iteration, see Figure 4, (a-c) for  $\lambda_0 = 1$ , and (d-f) for  $\lambda_0 = 10$ , respectively. As is noticed before, the single-particle excitation has a two-fold degeneracy for excitation at momentum  $p = 2\pi/L(1, 3)$  due to the boundary condition of the momentum. For the degenerate states, we compare the state fidelity in the subspace of the degenerate states. From the simulation results, we can find that the eigenstates obtained from the variational algorithms can be found with a high state fidelity, verifying the effectiveness of the variational algorithms.

Figure 4, (c,f) shows the state fidelity in the one-particle subspace. Here, the one-particle subspace is obtained by adiabatically evolving the one-particle state in the free theory. In the adiabatic evolution, we set the time step  $dt = 0.01$  and total time  $T = 50$  to ensure the state fidelity error below  $10^{-4}$ . The results indicate a high state overlap in this one-particle space in the presence of interaction  $\lambda_0 = 1$  and  $\lambda_0 = 10$ , consistent with our analysis.

We then discuss the simulation in the spectral crowding regime with a relatively small static mass  $m_0$ , where the many-particle state occupied at zero momentum  $p = 0$  will have lower energies compared to the single-particle state. In this regime, we should note that the excitations in the interacting field will not be local and may not have a well-defined particle number as that in the free theory. Therefore, searching for the excited state could be difficult in general, even when we could have access to adiabatic evolution. In what follows, we will discuss the low-lying excited states for two static mass  $m_0 = 0.5$  and  $m_0 = 0.37$ , and show the search for eigenstates using the

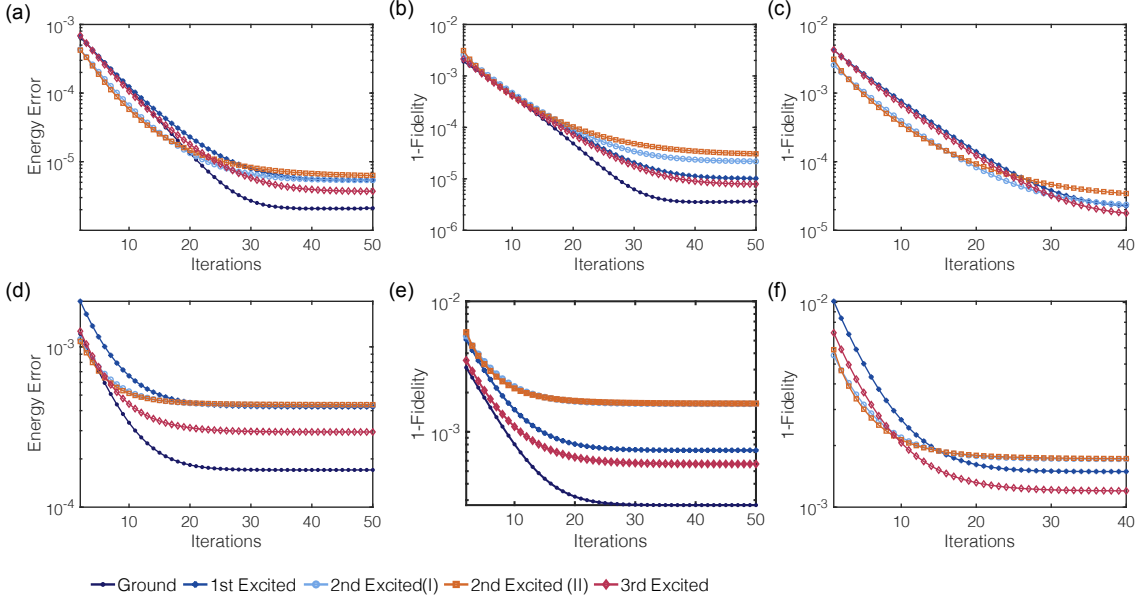


FIG. 4. Convergence towards the ground state and excited states of  $\lambda\phi^4$  theory in the momentum space using variational algorithms. The static mass is set to be  $m_0 = 1.27$ . Figure (a-c) corresponds to  $\lambda_0 = 1$  and Figure (d-f) corresponds to  $\lambda_0 = 10$ , respectively. The initial state for the excited states searching is the corresponding single-particle excited states of the free Hamiltonian  $\lambda_0 = 0$ . The error of the results with exact diagonalization. (a,d) We show the relative energy error of the ground state and the low-lying excited states. (b,e) We show the fidelity error of the ideal eigenstates and the simulated variational states. (d,f) The fidelity error of the first four excited states in a one-particle subspace.

variational algorithms.

Here, we represent the state as

$$|\psi_0\rangle = |n_0, n_1, n_2, n_3\rangle, \quad (62)$$

where  $n_j$  denotes the occupation number at the momentum  $p = \frac{2\pi j}{L}$ .

Let us first consider  $m_0 = 0.5$ . In this regime, the first five excited states of the free Hamiltonian are

$$|1, 0, 0, 0\rangle, |2, 0, 0, 0\rangle, |0, 1, 0, 0\rangle, |0, 0, 1, 0\rangle, |3, 0, 0, 0\rangle. \quad (63)$$

Compared to the case of  $m_0 = 1.37$ , the two-particle states have lower energies than the single-particle state, and the state  $|0, 0, 1, 0\rangle$  is indeed a highly excited state (higher than three-particle states). The excited states of the interacting Hamiltonian with  $\lambda_0 = 1$  follows the same order as that of the free Hamiltonian. We compare the simulation results for  $\lambda_0 = 1$  using the variational methods and adiabatic evolution in Figure 5.

Figure 5, (a,b) and (c,d) shows the results using variational methods and adiabatic evolution, respectively. Overall, the low-lying eigenstates obtained from the variational algorithms can be found with a high state fidelity.

In the strongly coupling regime, the two-particle excitation  $|2, 0, 0, 0\rangle$  for the interacting Hamiltonian with  $\lambda_0 = 10$  has higher energies compared to all the single-particle excitation, and it is even higher than the three-particle excitation  $|3, 0, 0, 0\rangle$ . Therefore, we choose to

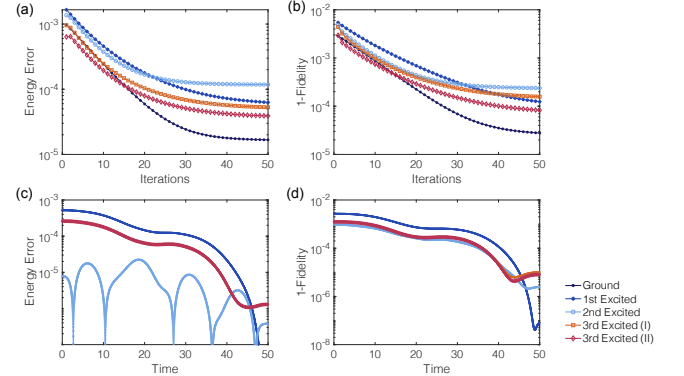


FIG. 5. The ground state and excited states preparation of  $\lambda\phi^4$  theory in the momentum space. The static mass is  $m_0 = 0.5$  and the interacting strength is  $\lambda_0 = 1$ . The initial state for the excited states searching is the corresponding low-lying excited states of the free Hamiltonian  $\lambda_0 = 0$ . (a,b) The convergence towards the ground state and excited states of  $\lambda\phi^4$  theory in the momentum space. (a) The energy error towards iteration. (b) The fidelity error towards iteration. (c,d) The energy error (c) and the fidelity error (d) under adiabatic evolution from the initial state.

prepare the single-particle excited states in the free theory as the initial states,

$$|1, 0, 0, 0\rangle, |0, 1, 0, 0\rangle, |0, 0, 0, 1\rangle, |0, 0, 1, 0\rangle. \quad (64)$$

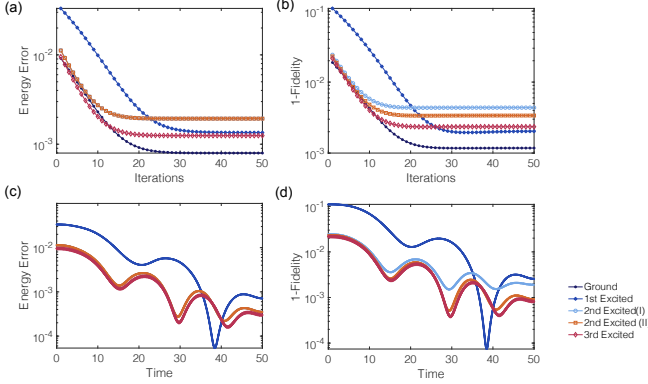


FIG. 6. The static mass is  $m_0 = 0.5$  and the interacting strength is  $\lambda_0 = 10$ . The initial state for the excited states searching is the single-particle excited states of the free Hamiltonian  $\lambda_0 = 0$ . (a) The energy error towards iteration. (b) The fidelity error towards iteration. (c,d) The energy error (c) and the fidelity error (d) under adiabatic evolution from the initial state.

Then, we use the variational quantum algorithms to search for the low-lying excited states. We show the simulation results with variational methods and adiabatic evolution for  $\lambda_0 = 10$  in Figure 6. Figure 6 shows that we could still use the excited state of the free Hamiltonian as the initial guess and obtain the target state with relatively high fidelity.

In the interacting theory, the single-particle excitation may not be well defined, and the eigenstate of the free theory may not be adequate for finding the ground state in the interacting theory, especially for the large interacting field  $\lambda_0 = 10$ . Note that the problem for the choice of the initial state exists in the adiabatic evolution.

Similarly, we could consider  $m_0 = 0.37$ , with the first five excited states of the free Hamiltonian as

$$|1,0,0,0\rangle, |2,0,0,0\rangle, |3,0,0,0\rangle, |0,1,0,0\rangle, |0,0,0,1\rangle. \quad (65)$$

We first show the convergence towards iteration in Figure 7 for  $\lambda_0 = 1$  for both the variational state preparation and adiabatic state preparation.

Similar to the case of  $m_0 = 0.5$ , the two-particle excitation for  $m_0 = 0.37$  has a small energy in the free theory, but it has a much higher energy compared to all the single-particle excitations and even higher than the three-particle excitation in the strong coupling regime. For instance, for a large interaction strength  $\lambda_0 = 10$ , the energy has the following relation

$$E(|3,0,0,0\rangle) < E(|0,0,1,0\rangle) < E(|2,0,0,0\rangle), \quad (66)$$

which indicates the energy single-particle excitation is between the multi-particle excitation in the interacting field. However, in the interacting field, we can find that the single-particle state is actually much close to the excited states in terms of state fidelity. Therefore, we similarly choose the initial states as the single-particle excited states.

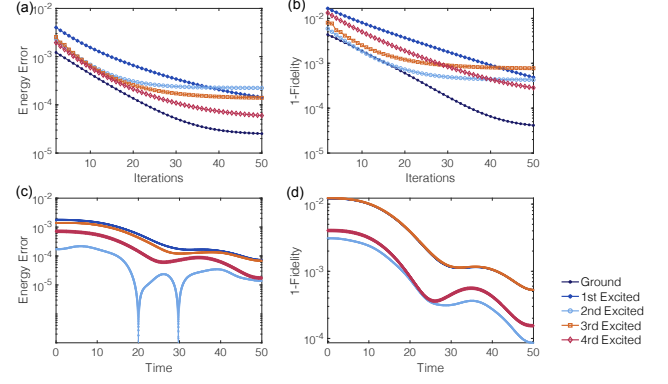


FIG. 7. The static mass is  $m_0 = 0.37$  and the interacting strength is  $\lambda_0 = 1$ . The initial state for the excited states searching is the corresponding low-lying excited states of the free Hamiltonian  $\lambda_0 = 0$ . (a,b) The convergence towards the ground state and excited states. (a) The energy error towards iteration. (b) The fidelity error towards iteration. (c,d) The energy error (c) and the fidelity error (d) under adiabatic evolution from the initial state.

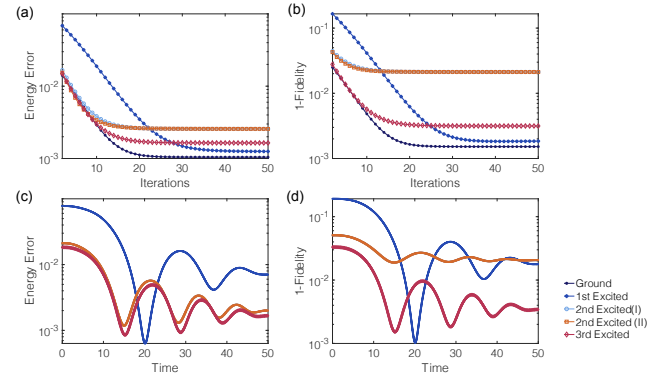


FIG. 8. The static mass is  $m_0 = 0.37$  and the interacting strength is  $\lambda_0 = 10$ . The initial state for the excited states searching is the corresponding single-particle excited states of the free Hamiltonian  $\lambda_0 = 0$ . (a) The energy error towards iteration. (b) The fidelity error towards iteration. (c,d) The energy error (c) and the fidelity error (d) under adiabatic evolution from the initial state.

We show the convergence towards iteration in Figure 8 for  $\lambda_0 = 10$ . As shown in Figure 8 (b,d), we can find that the state fidelity of the second excited state and the third excited state are relatively lower than the others. This is because these two states are actually evolved from the two degenerate states due to the boundary condition in the momentum space. However, the state fidelity in the subspace spanned by the degenerate states is numerically tested to be over 99%.

## VII. OUTLOOKS

In this paper, we discuss constructions of a variational version of the Jordan-Lee-Preskill algorithm in the near-term quantum computer. We justify the validity of the algorithm by several numerical simulations. We believe that our hybrid quantum-classical algorithm will eventually benefit possible solutions to open problems in fundamental physics, and benchmark tasks of near-term quantum devices. Here, we summarize some potential research directions along our path.

### A. Relation to the physical observables

In the previous discussions, we demonstrate the numerical simulation with fixed lattice spacing and lattice sites. To obtain the expectation value of physical observables in the real scalar field, say  $\langle \phi \rangle$ , we can first measure the expectation value with a series of increasing number of sites  $N$ ,  $\langle \phi_{a,N}^{(0)} \rangle$ , and extrapolate to the infinite volume limit  $N \rightarrow \infty$ ,  $\langle \phi_{a,N \rightarrow \infty}^{(0)} \rangle$ . Then, we further extrapolate these results to the continuum limit  $a \rightarrow 0$ ,  $\langle \phi^{(0)} \rangle \equiv \langle \phi_{a \rightarrow 0, N \rightarrow \infty}^{(0)} \rangle$ . Finally, we renormalize the expectation value as  $\langle \phi^{(R)} \rangle = Z \langle \phi^{(0)} \rangle$  with the renormalization constant  $Z$ . We leave the discussions to future work.

### B. Simulating quantum field theories in the NISQ era

Our work opens up a new direction of formulating several quantum field theory tasks in the setup of variational quantum simulation. In the era of noisy intermediate-scale quantum (NISQ), we expect that hybrid, variational quantum simulation algorithms might be one of the most accessible ways regarding near-term quantum hardware.

There is a landscape of quantum field theories with a full basket of open problems, who are looking for the potential computational capacity of quantum devices. Our work about strongly-coupled  $\lambda\phi^4$  theory is one of the simplest examples, whose non-perturbative nature is not fully understood by quantum field theorists. One could consider generalizing the scattering paradigm and its relevant techniques towards other quantum field theories. Specifically, lattice gauge theories in the four dimensions are particularly important for particle physicists, since it is related to quantum chromodynamics (QCD) and the Standard Model in particle physics. We refer to Refs. [25, 26, 28, 29, 52–55] for recent theoretical and experiment advances in the quantum simulation of lattice gauge field theories. One could look for other strongly-coupled quantum field theory problems, for instance, phase transitions in the finite-temperature

quantum field theories that are closely related to nuclear physics [4, 56].

### C. Identifying possible quantum advantages

Variational algorithms running on near-term devices might have further advantages for fundamental studies in quantum information science. Specifically, since we could design hybrid quantum-classical algorithms, it is easy for us to diagnose which classical or quantum steps have advantages practically. Although in this work, we do not focus on this comparison, we expect that similar comparisons could be performed in future studies. In the future, people might work out practically, which steps in the whole algorithms might have the quantum advantage, and if so, how much advantage they will have. Those studies might be helpful to construct the most useful quantum algorithms using practical experiences, and use those experiences to benchmark near-term devices. Quantum simulation of quantum field theories is a field that is still young, but we expect that finally, more techniques and hardcore developments could be formulated (see some similar analysis in computational quantum chemistry [57]).

### D. Error mitigation

In this paper, we neglected errors from device imperfections and shot noise from finite measurement samples. Those errors could accumulate and affect the simulation accuracy. Fortunately, various error mitigation techniques have been developed to suppress device errors [14, 15, 58–67]. By properly post-processing measurement results from different circuit realizations (e.g., with different noise ratios or symmetries), one can suppress the effect of noise by several orders [60, 68–70]. For instance, the  $\lambda\phi^4$  field preserves the reflection symmetry, so one can project the quantum state in the symmetry-protected subspace (see, e.g., [14, 58, 60]).

Meanwhile, the effect of shot noise could be reduced as well by exploiting more advanced measurement schemes [71–81]. The basic idea is to either exploit observable compatibility, importance sampling, or additional quantum circuit to more efficiently measure observables. Combining those error mitigation and advanced measurement schemes, we might be able to demonstrate our algorithms with current or near-term quantum hardware.

## VIII. ACKNOWLEDGEMENTS

Acknowledgements.—This paper is mostly finished when JL is a graduate student in Caltech. We thank Alex J. Buser, Liang Jiang, Natalie Klco, Peter Love, Ash Milsted, John Preskill, Burak Sahinoglu, Guifre

Vidal, and Xiaoyang Wang for related discussions. JL is supported in part by the Institute for Quantum Information and Matter (IQIM), an NSF Physics Frontiers Center (NSF Grant PHY-1125565) with support from the Gordon and Betty Moore Foundation (GBMF-2644), the Walter Burke Institute for Theoretical Physics. JL is also supported in part by International Business Machines (IBM) Quantum through the Chicago Quantum Exchange. XY acknowledges support from the Simons Foundation.

Note added.—Around the time when this research is finished, the papers [82, 83] appear, which has some overlaps with discussions in our paper, including the field bases [82] and quantum simulation using qudits [83].

### Appendix A: $\phi^4$ theory as an effective field theory

In this appendix, we simply review how the effective description of the classical Ising model in the long distance could be given by field theories, for the convenience of the quantum information science community. The observation where field theory could serve as an effective description of many-body physics has an important significance in theoretical physics, sharpening the importance of simulating quantum field theories.

The  $\phi^4$  field is one of the simplest interacting field theories related to the emergent behavior in the physical systems. In this section, we will review that the  $d$ -dimensional classical Ising model can be described by the  $\phi^4$  field at the long distance, following the discussions in [84] rather closely.

The classical magnetism can be described by the Hamiltonian

$$H = \sum_{ij} J_{ij} S_i S_j - \sum_i h_i S_i, \quad (\text{A1})$$

where  $J_{ij}$  is a translationally invariant correlation matrix describing the interaction of the spins. The classical partition function can be written as

$$\mathcal{Z} = \sum_{\{S_i\}} e^{\sum_{ij} \tilde{J}_{ij} S_i S_j + \sum_i h_i S_i}, \quad (\text{A2})$$

where we define  $\tilde{J} \equiv -\beta J$  and  $\tilde{h}_i \equiv \beta h_i$ .

By introducing a continuous auxiliary field  $\psi_i$ , the partition function is given by

$$\mathcal{Z} = \mathcal{N} \int D\psi \sum_{\{S_i\}} e^{-\frac{1}{4} \sum_{ij} \psi_i [\tilde{J}^{-1}]_{ij} \psi_j + \sum_i S_i (\psi_i + h_i)}, \quad (\text{A3})$$

where the Gaussian integral has been evaluated as

$$\begin{aligned} & \int Dv(x) \times \\ & \exp \left[ -\frac{1}{2} \int dx dx' v(x) A(x, x') v(x') + \int dx j(x) v(x) \right] \\ & \propto (\det A)^{-1/2} \exp \left[ \frac{1}{2} \int dx dx' j(x) A^{-1}(x, x') j(x') \right]. \end{aligned}$$

The equation above is under the saddle point approximation, which we preserves the second order of the functional

$$S[x] = S[\bar{x} + y] = S[\bar{x}] + \frac{1}{2} \int dt \int dt' y(t') A(t, t') y(t), \quad (\text{A4})$$

The partition function can now be written as [85]

$$\mathcal{Z} = \mathcal{N} \int D\psi \sum_{\{S_i\}} e^{-\frac{1}{2} \sum_{ij} \psi_i [\tilde{J}^{-1}]_{ij} \psi_j + \sum_i S_i (\sqrt{2}\psi_i + h_i)}. \quad (\text{A5})$$

Note that the interaction between spins is decoupled by the continuous auxiliary field. In this case, we could work with the multi-dimensional integral  $\int D\psi$  instead of the summation over discretized spins

$$\mathcal{Z} = \mathcal{N} \int D\psi e^{-\frac{1}{2} \sum_{ij} (\psi_i - h_i) \tilde{J}_{ij}^{-1} (\psi_j - h_j) + \sum_i \ln(\cosh \sqrt{2}\psi_i)}, \quad (\text{A6})$$

where we have used  $S_i = \pm 1$ , and the normalization factor has absorbed the trivial prefactor. Notice that

$$\ln \cosh(x) = \frac{1}{2} x^2 - \frac{1}{12} x^4 + \dots$$

So the Ising model could be described by the  $\phi_4$  theory at the long distance.

To make the fourth-order term more clear, we change the integration variable  $\psi$  to the field variable via

$$\phi_i \equiv \frac{1}{\sqrt{2}} \sum_j \tilde{J}_{ij}^{-1} \psi_j, \quad (\text{A7})$$

and we have

$$\mathcal{Z} = \mathcal{N} \int D\phi e^{-\sum_{ij} \phi_i \tilde{J}_{ij} \phi_j + \sum_i \phi_i h_i + \sum_i \ln \cosh(2 \sum_j \tilde{J}_{ij} \phi_j)}. \quad (\text{A8})$$

We note that the amplitude of the field  $\phi$  indicates a measure of magnetism. If the coupling is transnational invariant, which indicates a spatially smooth field, we can capture this feature by the Fourier transformation:

$$\phi_i = \frac{1}{\sqrt{N}} \sum_{\mathbf{k}} e^{-i\mathbf{k} \cdot \mathbf{r}_i} \phi(\mathbf{k}). \quad (\text{A9})$$

Given the expansion

$$(\tilde{J}\phi)(\mathbf{k}) = \tilde{J}(\mathbf{k})\phi(\mathbf{k}) = \tilde{J}_0 \phi(\mathbf{k}) + \frac{1}{2} \mathbf{k}^2 \tilde{J}_0'' \phi(\mathbf{k}) + \mathcal{O}(\mathbf{k}^4), \quad (\text{A10})$$

the effective action in the momentum space up to the fourth order is given by

$$S[\phi] = \sum_{\mathbf{k}} [\phi_{\mathbf{k}} (c_1 + c_2 \mathbf{k}^2) \phi_{-\mathbf{k}} + c_3 \phi_{\mathbf{k}} h_{-\mathbf{k}}] + c_4 \sum_{\mathbf{k}_1, \dots, \mathbf{k}_4} \phi_{\mathbf{k}_1} \phi_{\mathbf{k}_2} \phi_{\mathbf{k}_3} \phi_{-\mathbf{k}_1 - \mathbf{k}_2 - \mathbf{k}_3} (\mathbf{k}^4, h^2, \phi^6), \quad (\text{A11})$$

where

$$\begin{aligned} c_1 &= \tilde{J}_0(1 - 2\tilde{J}_0), \\ c_2 &= \frac{1}{2}\tilde{J}_0''(1 - 4\tilde{J}_0), \\ c_3 &= 1, \end{aligned} \quad (\text{A12})$$

which can be determined from the interaction coupling. We can thus see its correspondence to (17), the  $\phi^4$  field in the momentum space.

In the real space, the effective action admits the form of  $\phi^4$  field as

$$S[\phi] = \int d^d x c_1 \phi^2 + c_2 (\partial \phi)^2 + c_3 \phi h + c_4 \phi^4. \quad (\text{A13})$$

When the coupled external field is zero, i.e.,  $h = 0$ , it becomes the prototypical  $\phi^4$  field discussed in the main text. Suppose  $c_2 > 0$ , for  $c_1 > 0$ , the action has a global minimum at  $\phi = 0$ , and thus the ground state is in the paramagnetic phase. While for  $c_1 < 0$ , the action has two degenerate minima. Thus the phase is spontaneously broken with a ferromagnetic ordering. If the interaction strength  $J_{ij} < 0$ , the constant  $c_1$  is positive at sufficiently low temperature, and it becomes zero at the transition temperature. Therefore, the  $\phi^4$  field could capture the critical behavior of the paramagnetic phase to the ferromagnetic phase.

---

[1] J. Preskill, *Quantum* **2**, 79 (2018).

[2] F. Arute, K. Arya, R. Babbush, D. Bacon, J. C. Bardin, R. Barends, R. Biswas, S. Boixo, F. G. Brandao, D. A. Buell, *et al.*, *Nature* **574**, 505 (2019).

[3] R. P. Feynman, *Int. J. Theor. Phys.* **21** (1982).

[4] J. Preskill, PoS **LATTICE2018**, 024 (2018), arXiv:1811.10085 [hep-lat].

[5] J. Liu, *Does Richard Feynman Dream of Electric Sheep? Topics on Quantum Field Theory, Quantum Computing, and Computer Science*, Ph.D. thesis, Caltech (2021).

[6] S. P. Jordan, K. S. Lee, and J. Preskill, *Science* **336**, 1130 (2012), arXiv:1111.3633 [quant-ph].

[7] S. P. Jordan, K. S. Lee, and J. Preskill, *Quant. Inf. Comput.* **14**, 1014 (2014), arXiv:1112.4833 [hep-th].

[8] A. Milsted, J. Liu, J. Preskill, and G. Vidal, (2020), arXiv:2012.07243 [quant-ph].

[9] A. Peruzzo, J. McClean, P. Shadbolt, M.-H. Yung, X.-Q. Zhou, P. J. Love, A. Aspuru-Guzik, and J. L. O'Brien, *Nature Communications* **5** (2014), 10.1038/ncomms5213.

[10] E. Farhi, J. Goldstone, and S. Gutmann, arXiv preprint arXiv:1411.4028 (2014).

[11] J. R. McClean, J. Romero, R. Babbush, and A. Aspuru-Guzik, *New Journal of Physics* **18**, 023023 (2016).

[12] Y. Li and S. C. Benjamin, *Physical Review X* **7**, 021050 (2017).

[13] X. Yuan, S. Endo, Q. Zhao, Y. Li, and S. C. Benjamin, *Quantum* **3**, 191 (2019).

[14] S. Endo, Z. Cai, S. C. Benjamin, and X. Yuan, *Journal of the Physical Society of Japan* **90**, 032001 (2021), <https://doi.org/10.7566/JPSJ.90.032001>.

[15] M. Cerezo, A. Arrasmith, R. Babbush, S. C. Benjamin, S. Endo, K. Fujii, J. R. McClean, K. Mitarai, X. Yuan, L. Cincio, and P. J. Coles, *Nature Reviews Physics* **3**, 625 (2021).

[16] Z.-J. Zhang, J. Sun, X. Yuan, and M.-H. Yung, arXiv preprint arXiv:2011.05283 (2020).

[17] S. Endo, J. Sun, Y. Li, S. C. Benjamin, and X. Yuan, *Phys. Rev. Lett.* **125**, 010501 (2020).

[18] X. Xu, J. Sun, S. Endo, Y. Li, S. C. Benjamin, and X. Yuan, *Science Bulletin* (2021), <https://doi.org/10.1016/j.scib.2021.06.023>.

[19] S. McArdle, T. Jones, S. Endo, Y. Li, S. C. Benjamin, and X. Yuan, *npj Quantum Information* **5**, 1 (2019).

[20] S. McArdle, A. Mayorov, X. Shan, S. Benjamin, and X. Yuan, *Chem. Sci.* **10**, 5725 (2019).

[21] P. O'Malley, R. Babbush, I. Kivlichan, J. Romero, J. McClean, R. Barends, J. Kelly, P. Roushan, A. Tranter, N. Ding, and et al., *Physical Review X* **6** (2016), 10.1103/physrevx.6.031007.

[22] Y. Shen, X. Zhang, S. Zhang, J.-N. Zhang, M.-H. Yung, and K. Kim, *Physical Review A* **95** (2017), 10.1103/physreva.95.020501.

[23] A. M. Childs, Y. Su, M. C. Tran, N. Wiebe, and S. Zhu, arXiv preprint arXiv:1912.08854 (2019).

[24] G. H. Low and I. L. Chuang, arXiv preprint arXiv:1610.06546 (2016).

[25] A. F. Shaw, P. Lougovski, J. R. Stryker, and N. Wiebe, *Quantum* **4**, 306 (2020).

[26] B. Chakraborty, M. Honda, T. Izubuchi, Y. Kikuchi, and A. Tomiya, “Digital quantum simulation of the schwinger model with topological term via adiabatic state preparation,” (2020), arXiv:2001.00485 [hep-lat].

[27] J. Bender, E. Zohar, A. Farace, and J. I. Cirac, *New Journal of Physics* **20**, 093001 (2018).

[28] C. Kokail, C. Maier, R. van Bijnen, T. Brydges, M. K. Joshi, P. Jurcevic, C. A. Muschik, P. Silvi, R. Blatt, C. F. Roos, *et al.*, *Nature* **569**, 355 (2019).

[29] D. Paulson, L. Dellantonio, J. F. Haase, A. Celi, A. Kan, A. Jena, C. Kokail, R. van Bijnen, K. Jansen, P. Zoller, and et al., *PRX Quantum* **2** (2021), 10.1103/prxquantum.2.030334.

[30] A. Kitaev and W. A. Webb, arXiv preprint arXiv:0801.0342 (2008).

[31] J. Liu and Y. Xin, *JHEP* **12**, 011 (2020), arXiv:2004.13234 [hep-th].

[32] H. Gharibyan, M. Hanada, M. Honda, and J. Liu, *JHEP*

**07**, 140 (2021), arXiv:2011.06573 [hep-th].

[33] A. Buser, H. Gharibyan, M. Hanada, M. Honda, and J. Liu, (2020), arXiv:2011.06576 [hep-th].

[34] E. Rinaldi, X. Han, M. Hassan, Y. Feng, F. Nori, M. McGuigan, and M. Hanada, (2021), arXiv:2108.02942 [quant-ph].

[35] M. Kreshchuk, W. M. Kirby, G. Goldstein, H. Beauchemin, and P. J. Love, (2020), arXiv:2002.04016 [quant-ph].

[36] M. Kreshchuk, S. Jia, W. M. Kirby, G. Goldstein, J. P. Vary, and P. J. Love, Phys. Rev. A **103**, 062601 (2021), arXiv:2011.13443 [quant-ph].

[37] M. Kreshchuk, S. Jia, W. M. Kirby, G. Goldstein, J. P. Vary, and P. J. Love, Entropy **23**, 597 (2021), arXiv:2009.07885 [quant-ph].

[38] A. Macridin, P. Spentzouris, J. Amundson, and R. Harnik, Phys. Rev. A **98**, 042312 (2018), arXiv:1805.09928 [quant-ph].

[39] N. Klio and M. J. Savage, Phys. Rev. A **99**, 052335 (2019), arXiv:1808.10378 [quant-ph].

[40] N. P. Sawaya, T. Menke, T. H. Kyaw, S. Johri, A. Aspuru-Guzik, and G. G. Guerreschi, npj Quantum Information **6**, 1 (2020).

[41] The Hamiltonian with truncated energy levels is represented in a low-energy subspace.

[42] P. J. Ollitrault, A. Baiardi, M. Reiher, and I. Tavernelli, Chemical science **11**, 6842 (2020).

[43] J. Stokes, J. Izaac, N. Killoran, and G. Carleo, Quantum **4**, 269 (2020).

[44] M. Motta, C. Sun, A. T. Tan, M. J. O'Rourke, E. Ye, A. J. Minnich, F. G. Brandão, and G. K.-L. Chan, Nature Physics **16**, 205 (2020).

[45] K. A. Landsman, Y. Wu, P. H. Leung, D. Zhu, N. M. Linke, K. R. Brown, L. Duan, and C. Monroe, Physical Review A **100**, 022332 (2019).

[46] However, for this set of parameter choices, the energies of two-particle and three-particle zero-momentum states are lower than the single-particle excited states.

[47] L. Vanderstraeten, J. Haegeman, and F. Verstraete, SciPost Physics Lecture Notes (2019).

[48] There are some recent research about quantum simulation in the low energy subspace, see Ref. [? ].

[49] X. Yuan, J. Sun, J. Liu, Q. Zhao, and Y. Zhou, Phys. Rev. Lett. **127**, 040501 (2021).

[50] J. Sun, S. Endo, H. Lin, P. Hayden, V. Vedral, and X. Yuan, arXiv preprint arXiv:2106.05938 (2021).

[51] For sufficiently small  $\lambda_0$ , the eigenstates in the free theory is close to that in the interacting theory.

[52] T. Farrelly and J. Streich, “Discretizing quantum field theories for quantum simulation,” (2020), arXiv:2002.02643 [quant-ph].

[53] H. Lamm, S. Lawrence, Y. Yamauchi, N. Collaboration, *et al.*, Physical Review D **100**, 034518 (2019).

[54] P. Hauke, D. Marcos, M. Dalmonte, and P. Zoller, Physical Review X **3**, 041018 (2013).

[55] F. M. Surace, P. P. Mazza, G. Giudici, A. Lerose, A. Gambassi, and M. Dalmonte, Physical Review X **10**, 021041 (2020).

[56] Y. Alexeev *et al.*, (2020), arXiv:1912.07577 [quant-ph].

[57] V. von Burg, G. H. Low, T. Häner, D. S. Steiger, M. Reiher, M. Roetteler, and M. Troyer, arXiv preprint arXiv:2007.14460 (2020).

[58] J. R. McClean, M. E. Kimchi-Schwartz, J. Carter, and W. A. de Jong, Phys. Rev. A **95** (2017).

[59] Y. Li and S. C. Benjamin, Phys. Rev. X **7**, 021050 (2017).

[60] X. Bonet-Monroig, R. Sagastizabal, M. Singh, and T. O’Brien, Physical Review A **98**, 062339 (2018).

[61] K. Temme, S. Bravyi, and J. M. Gambetta, Phys. Rev. Lett. **119**, 180509 (2017).

[62] S. Endo, S. C. Benjamin, and Y. Li, Physical Review X **8**, 031027 (2018).

[63] J. I. Colless, V. V. Ramasesh, D. Dahmen, M. S. Blok, M. E. Kimchi-Schwartz, J. R. McClean, J. Carter, W. A. de Jong, and I. Siddiqi, Phys. Rev. X **8** (2018).

[64] M. Otten and S. Gray, Physical Review A **99**, 012338 (2019).

[65] S. Endo, Q. Zhao, Y. Li, S. Benjamin, and X. Yuan, Phys. Rev. A **99**, 012334 (2019).

[66] S. McArdle, X. Yuan, and S. Benjamin, Physical review letters **122**, 180501 (2019).

[67] J. Sun, X. Yuan, T. Tsunoda, V. Vedral, S. C. Benjamin, and S. Endo, Phys. Rev. Applied **15**, 034026 (2021).

[68] A. Kandala, K. Temme, A. D. Córcoles, A. Mezzacapo, J. M. Chow, and J. M. Gambetta, Nature **567**, 491 (2019).

[69] G. A. Quantum, Collaborators, F. Arute, K. Arya, R. Babbush, D. Bacon, J. C. Bardin, R. Barends, S. Boixo, M. Broughton, B. B. Buckley, D. A. Buell, B. Burkett, N. Bushnell, Y. Chen, Z. Chen, B. Chiaro, R. Collins, W. Courtney, S. Demura, A. Dunsworth, E. Farhi, A. Fowler, B. Foxen, C. Gidney, M. Giustina, R. Graff, S. Habegger, M. P. Harrigan, A. Ho, S. Hong, T. Huang, W. J. Huggins, L. Ioffe, S. V. Isakov, E. Jeffrey, Z. Jiang, C. Jones, D. Kafri, K. Kechedzhi, J. Kelly, S. Kim, P. V. Klimov, A. Korotkov, F. Kostritsa, D. Landhuis, P. Laptev, M. Lindmark, E. Lucero, O. Martin, J. M. Martinis, J. R. McClean, M. McEwen, A. Megrant, X. Mi, M. Mohseni, W. Mruczkiewicz, J. Mutus, O. Naaman, M. Neeley, C. Neill, H. Neven, M. Y. Niu, T. E. O’Brien, E. Ostby, A. Petukhov, H. Putterman, C. Quintana, P. Roushan, N. C. Rubin, D. Sank, K. J. Satzinger, V. Smelyanskiy, D. Strain, K. J. Sung, M. Szalay, T. Y. Takeshita, A. Vainsencher, T. White, N. Wiebe, Z. J. Yao, P. Yeh, and A. Zalcman, Science **369**, 1084 (2020), <https://science.sciencemag.org/content/369/6507/1084.full.pdf>.

[70] Y. Kim, C. J. Wood, T. J. Yoder, S. T. Merkel, J. M. Gambetta, K. Temme, and A. Kandala, “Scalable error mitigation for noisy quantum circuits produces competitive expectation values,” (2021), arXiv:2108.09197 [quant-ph].

[71] A. Kandala, A. Mezzacapo, K. Temme, M. Takita, M. Brink, J. M. Chow, and J. M. Gambetta, Nature **549**, 242 (2017).

[72] B. Wu, J. Sun, Q. Huang, and X. Yuan, (2021), arXiv:2105.13091 [quant-ph].

[73] V. Verteletskyi, T.-C. Yen, and A. F. Izmaylov, The Journal of chemical physics **152**, 124114 (2020).

[74] C. Hadfield, S. Bravyi, R. Raymond, and A. Mezzacapo, arXiv preprint arXiv:2006.15788 (2020).

[75] G. Torlai, G. Mazzola, G. Carleo, and A. Mezzacapo, Physical Review Research **2**, 022060 (2020).

[76] H.-Y. Huang, R. Kueng, and J. Preskill, Nature Physics **16**, 1050 (2020).

[77] H.-Y. Huang, R. Kueng, and J. Preskill, arXiv preprint arXiv:2103.07510 (2021).

[78] J. Cotler and F. Wilczek, Physical Review Letters **124**, 100401 (2020).

- [79] C. Hadfield, arXiv e-prints , arXiv:2105.12207 (2021), arXiv:2105.12207 [quant-ph].
- [80] S. Hillmich, C. Hadfield, R. Raymond, A. Mezzacapo, and R. Wille, (2021), arXiv:2105.06932 [quant-ph].
- [81] T. Zhang, J. Sun, X.-X. Fang, X. Zhang, X. Yuan, and H. Lu, “Experimental quantum state measurement with classical shadows,” (2021), arXiv:2106.10190 [quant-ph].
- [82] A. Macridin, A. C. Y. Li, S. Mrenna, and P. Spentzouris, (2021), arXiv:2108.10793 [quant-ph].
- [83] D. M. Kurkcuoglu, M. S. Alam, A. C. Li, A. Macridin, and G. N. Perdue, arXiv preprint arXiv:2108.13357 (2021).
- [84] A. Altland and B. D. Simons, *Condensed matter field theory* (Cambridge university press, 2010).
- [85] The first order at the stationary point is zero because
$$\frac{\delta S[x]}{\delta x(t)} = 0|_{x=\bar{x}} . \quad (\text{A14})$$